

DEVELOPMENT OF UNNATURAL SUBSTRATES AND TRYPTOPHAN AMINO ACIDS
TO STUDY PROTON COUPLED ELECTRON TRANSFER IN ENZYMES

by

Kei Ohgo

December, 2020

Director of Thesis: Adam R. Offenbacher

Major Department: Chemistry

Proton-coupled electron transfer plays an important role in substrate oxidation by C-H bond cleavage and long-range pathways associated with bioenergetics. This thesis is focused on the synthesis of unnatural substrates and tryptophan amino acids to study these effects in enzyme reactions. The functionalization of C-H bonds is an important chemical transformation, representing a challenge in the design of asymmetric organometallic catalysts to generate a range of organic molecules with diverse functional groups. Soybean lipoxygenase-1 is a model enzyme system that catalyzes C-H activation reactions. Unnatural and volume-filling fatty acid derivatives were designed to test with a mutant soybean lipoxygenase that has an expanded active site. The goal of this strategy is to develop new hydroperoxide-based products of long-chain aliphatic compounds. Fluorinated 5-hydroxytryptophan (Fn-5HOW) derivatives were synthesized on a large scale using a chemoenzymatic approach. These redox-active Fn-5HOW derivatives exhibit tyrosine-like proton-bound oxidation and are associated with the spectroscopic characteristics of neutral radicals that are easily distinguishable from natural aromatic amino acids. As a proof of concept, these unnatural amino acids have been incorporated into structured peptides and model proteins. These unnatural fluorinated 5HOW derivatives may act as reporters for tryptophan-mediated biological electron transport.

DEVELOPMENT OF UNNATURAL SUBSTRATES AND TRYPTOPHAN AMINO ACIDS
TO STUDY PROTON COUPLED ELECTRON TRANSFER IN ENZYMES

A Thesis

Presented to Faculty of the Department of Chemistry

East Carolina University

In Partial Fulfillment of the Requirements for the Degree

Master of Science in Chemistry

by

Kei Ohgo

December, 2020

© Kei Ohgo, 2020

DEVELOPMENT OF UNNATURAL SUBSTRATES AND TRYPTOPHAN AMINO ACIDS
TO STUDY PROTON COUPLED ELECTRON TRANSFER IN ENZYMES

by
Kei Ohgo

APPROVED BY:

DIRECTOR OF

THESIS: _____

(Adam R. Offenbacher, Ph.D.)

COMMITTEE MEMBER: _____

(William E. Allen, Ph.D.)

COMMITTEE MEMBER: _____

(Brian E. Love, Ph.D.)

COMMITTEE MEMBER: _____

(Colin Burns, Ph.D.)

COMMITTEE MEMBER: _____

(Patrick J. Horn, Ph.D.)

CHAIR OF THE DEPARTMENT

OF CHEMISTRY: _____

(Andrew T. Morehead Jr., Ph.D.)

DEAN OF THE

GRADUATE SCHOOL: _____

(Paul J. Gemperline, Ph.D.)

ACKNOWLEDGEMENTS

I would like to express my appreciation for my Principle Investigator, Dr. Adam, Offenbacher, whose guidance and help made this possible. Also, I would like to thank my thesis committee members for their time and patience.

Finally, I would like to thank the Department of Chemistry and the Burroughs-Wellcome Foundation for creating this amazing and supportive team, and for helping me to get involved and adjusted to the new culture and new area of study.

TABLE OF CONTENTS

TITLE PAGE	i
COPYRIGHT PAGE.....	ii
SIGNATURE PAGE.....	iii
ACKNOWLEDGEMENT	iv
CHAPTER 1: INTRODUCTION	1
References.....	18
CHAPTER 2: DESIGN OF UNNATURAL, LIPOXYGENASE-TARGETEDSUBSTRATES TOWARDS NOVEL HYDROPEROXIDE FORMATION FROM BIOCATALYTIC C-H ACTIVATION.....	25
References.....	38
CHAPTER 3: DESIGN OF UNNATURAL TRYPTOPHAN AMINO ACID TO STUDY PROTON COUPLED ELECTRON TRANSFER.....	39
References.....	54
APPENDIX 1:SYNTHESIS OF OLEYL SULFATE AS AN ALLOSTERIC EFFECTOR FOR LIPOXYGENASES	55

Chapter 1

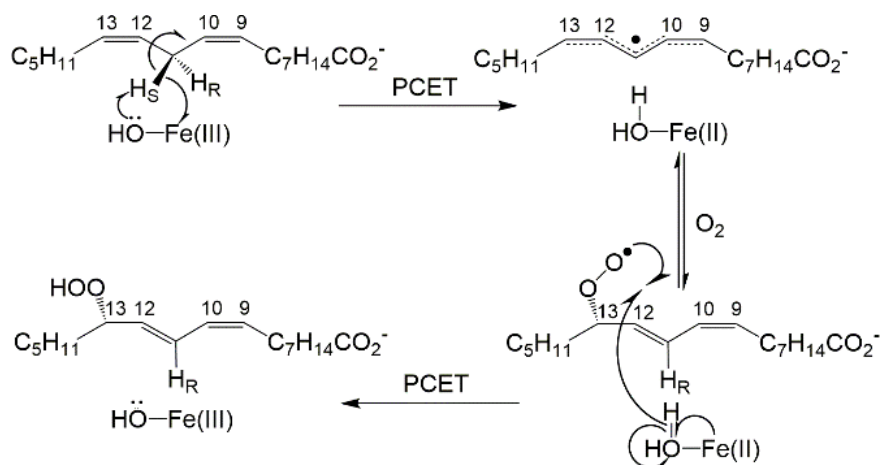
Introduction

1.1. Substrate oxidation by PCET: Enzyme C-H activation with unnatural substrates.

The field of C-H activation is expanding rapidly and aims to provide a sustainable approach for complex syntheses. Therefore, C-H functionalization has the potential for the petroleum industry to expand the usefulness of these refined oils and fuels. The mainstream approach to C-H catalyst design has focused on d-block transition metals.¹⁻⁶ While these catalysts provide highly desirable yields and synthetic controls, their limitations can include air sensitivity and toxicity in the reaction process. To overcome these limitations, researchers have begun developing and using biocatalysts,^{7,8} or natural enzymes that have activity for industrials relevant reactions.

1.1.1. Soybean lipoxygenase as a biocatalyst

Lipoxygenase (LOX) is an enzyme that catalyzes the regio- and stereospecific insertion of molecular oxygen into polyunsaturated fatty acids with the formation of fatty acid hydroperoxides. The reaction is initiated by proton-coupled electron transfer (PCET) in which C-H cleavage is mediated by a mononuclear non-heme metal (usually iron) hydroxide cofactor. (**Scheme 1.1**) In this cofactor, electrons are accepted at the Fe³⁺ center and protons are accepted at the metal bound hydroxide. As the C-H cleavage proceeds, delocalized organic radicals are formed, and the radicals are quenched by molecular oxygen. Reverse PCET leads to the release of oxidized fatty acids. Recently, plant soybean lipoxygenase (SLO) has begun to emerge as a potential biocatalyst due to its attractive properties.⁹ First is that the immediate hydroperoxide product of SLO has the chemical ability to form various secondary products by the addition of secondary enzymes (see the example in Figure 1.1).¹⁰ Second is that SLO is the most efficient lipoxygenase characterized, the C-H activation step completely determines the rate under optimal conditions (pH 9, 30°C). Third is that SLO is one of the most stereoselective and regio-selective LOX enzymes, 95% of the product representing (9Z,11E,13S)-13-hydroperoxyoctadeca-9,11-dienoic acid (13S-HpODE).¹¹ Finally, that even in the immobilized form, SLO has desirable reactivity at room temperature.



Scheme 1.1. Mechanism of fatty acid (linoleic acid) peroxidation by SLO. The C-H activation (first and rate-limiting) step occurs through a PCET mechanism.

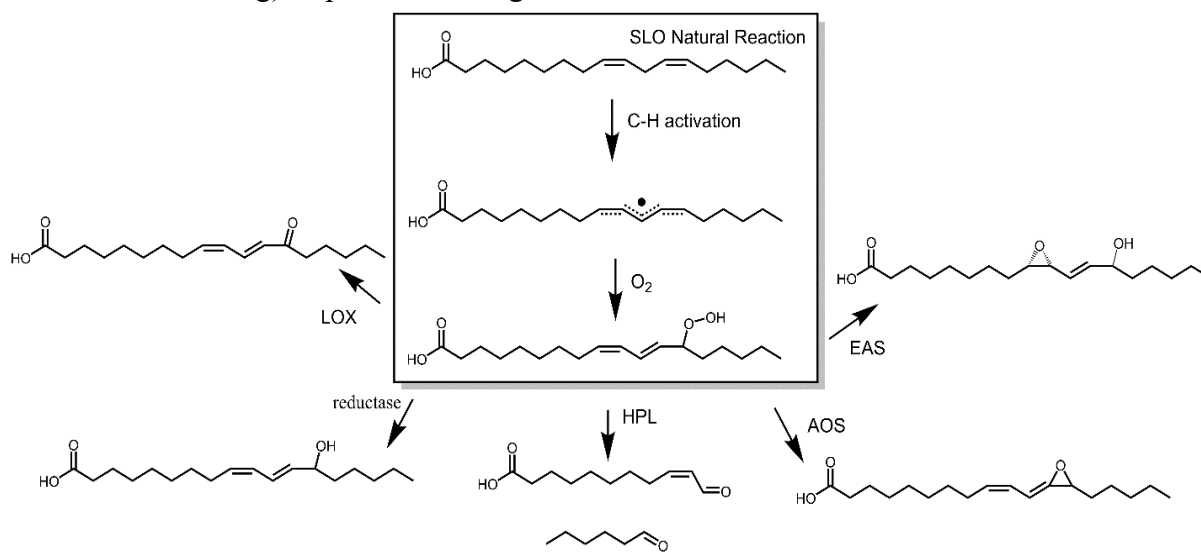


Figure 1.1. The hydroperoxide product, 13S-HpODE, of lipoxygenases is a precursor for numerous cell-signaling molecules from the additional enzymatic processing, shown by the arrows. Novel hydroperoxides could lead to development of new and useful small molecules.

1.1.2. Sample of unnatural substrates from literature

There are several reports of modified substrates for lipoxygenases (**Table 1.1**). However, these substrate analogs are typically limited to unsaturated acyl chains with carboxylic acid head functional groups, and only a few examples involving ring structures have emerged (compounds **3**, **5**, **6** and **7** in **table 1.1**). For compound **7**, the phenyl ring is expected to bind on the surface rather than entering the substrate biochemical. For compounds **3**, **5**, and **6**, lipoxygenase reactivity

is very low and usually correlates with weak binding (high K_m values). The substrate range of lipoxygenase has been limited to fatty acid derivatives due to the partially restricted hydrophobic substrate channels. A phenyl-based compound that binds to lipoxygenase is often a reduction inhibitor that replaces the bound oxygen atom of the ferric center catalyst.¹²

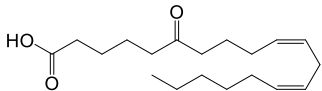
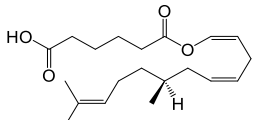
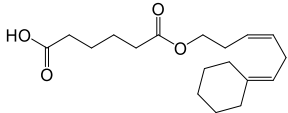
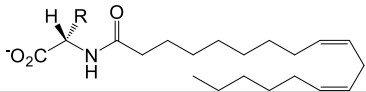
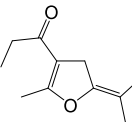
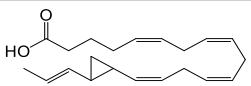
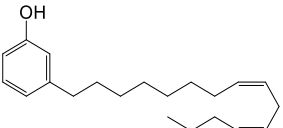
	Reactant	k_{cat} (s^{-1})	K_m (μM)
	LA ^{a,b}	225 (15)	30 (2)
1^{a,c}		97	50
2^{a,c}		4	370
3^{a,c}		2	150
4^{a,d}		182-205	8-9
5^e		$\ll 1^f$	N.D. ^g
6^h		$\ll 1^f$	N.D. ^g
7ⁱ		N.D. ^g	N.D. ^g

Table 1.1. SLO oxygenation of select non-natural substrates

^aConducted at 25°C and pH 9. ^bfrom ref.¹³ ^cfrom ref.¹⁴ ^dfrom ref.¹⁵; kinetic parameters for R = L and D-valine. ^efrom ref.¹⁶ ^fNo quantitative number possible but required hours. ^gN.D., not determined. ^hfrom ref.¹⁷; required 50 atm O₂ for reactivity.

1.1.3. Double mutant soybean lipoxygenase

A recent report of a "double mutant" (DM) SLO with an expanded active site cavity, determined by X-ray crystallography, might react with larger volume substrates such as phenyl

derivatives. This mutation in SLO generated from the co-mutation of two highly conserved leucine residues in the SLO active site of alanine (L546 and L754). The opened active site causes the substrate to relax back into the hydrophobic pocket (**Figure 1.2**).¹⁸ As a result, the reactive carbon of linoleic acid is more than 1 Ångstrom away from the hydrogen acceptor.¹⁹ The reduced activity of DMSLO on the natural substrate linoleic acid (reduced rate constant by 10⁴-fold)²⁰ raises questions about whether "volume-filled" substrates such as phenyl derivatives could function as effective substrates.

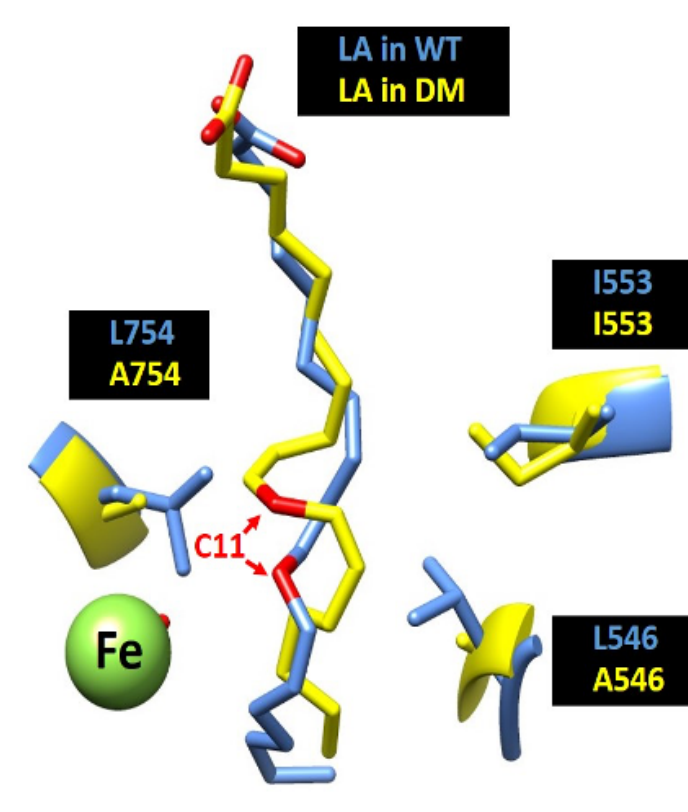


Figure 1.2. A comparison between the ground state substrate binding mode in wild type (blue) and DM (yellow). The reactive carbon C11 is colored as red, iron colored as green.¹⁸

1.2.1. Long-Range PCET with mediated in biological catalysis (RNR as Case Study)

One example for study of long-range PCET mediated by the tyrosine side chain is from ribonucleotide reductase (RNR), an enzyme involved in the reduction of ribonucleotides to deoxyribonucleotides, a precursor to DNA biosynthesis.²⁴ All organisms require DNA synthesis prior to cell division. For normal function (*i.e.* non-cancer) DNA synthesis requires a balanced supply of various deoxyribonucleotide triphosphates (dNTPs). The only biochemical pathway for de novo dNTP synthesis is a reaction catalyzed via the enzyme RNR. This reaction converts four ribonucleotide triphosphates (NTPs) to the corresponding dNTPs by reducing the C2'-OH bond. (Figure 1.5)^{22,25-27}

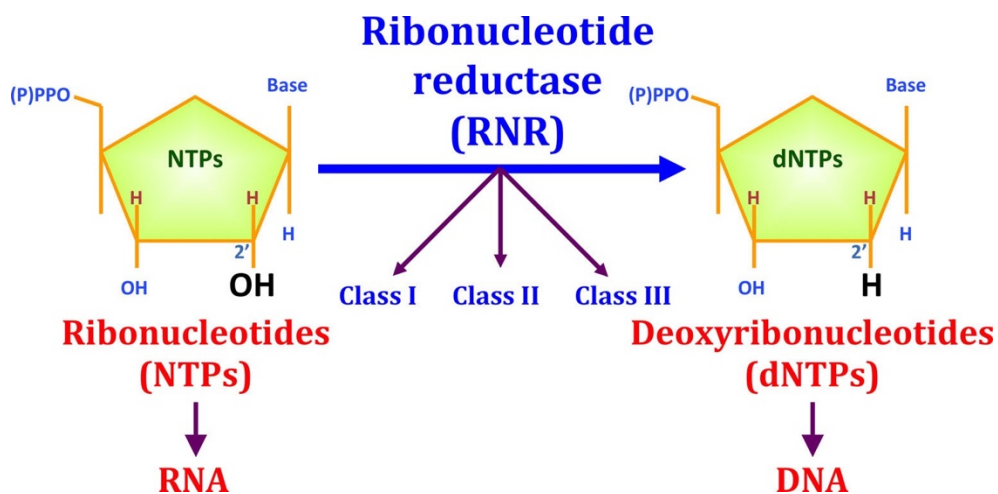


Figure 1.5. The reduction of ribonucleotides to deoxyribonucleotides by RNR. Three different RNR classes (I, II, and III) have been described for this enzyme family. RNR is important for evolution, as this enzyme played an important role during the transition from an RNA to a DNA world. RNR enzymes catalyze the reduction of the ribose C2'-OH to C2'-H.²²

Class I enzymes are oxygen dependent, and are found in practically all eukaryotic organisms, from yeast and algae to plants and mammals, and some prokaryotes and viruses also express this type. Class I is further divided into five subclasses. Ia and Ib are based on polypeptide sequence homologies and their overall allosteric regulation behavior. Class Ia exists in eukaryotes, prokaryotes, viruses, and bacteriophages, while Ib has only been found in prokaryotes.^{22,25,28} PCET in class I RNR, are mediated by tyrosyl radicals, which are tetrameric enzymes ($\alpha 2\beta 2$). The

tyrosine 122 (Y122) that is in *E. coli* numbering, forms a stable ($t_{1/2} \sim$ hours-days) tyrosyl radical though O_2 dependent activation. Y122• is responsible for oxidation active site cysteine 439 (C439), 35Å away that initiates catalysis. From $\alpha 2$ and $\beta 2$ structures, direct hydrogen atom transfer between Y122 and C439 is not feasible. Such a transfer requires multi step hopping of electron over 35Å from C439 to Y122•. Inspiration from a docked model²⁹ and the new trapped ‘catalytic’ cryoEM³⁰ structure shows a pathway of conserved tyrosine and tryptophan residues (**Figure 1.6**). Mutation of tyrosine residues along the pathway causes inactive enzymes.²⁹ This supports a role for tyrosines, however does not provide information on mechanism. Subsequent use of the unnatural amino acids, fluorotyrosine and nitrotyrosine, have provided confirmation of this pathway.²⁴ It is important to note that there remains no strong evidence for W48 in pathway because of, in part, a lack of viable tryptophan unnatural amino acids.

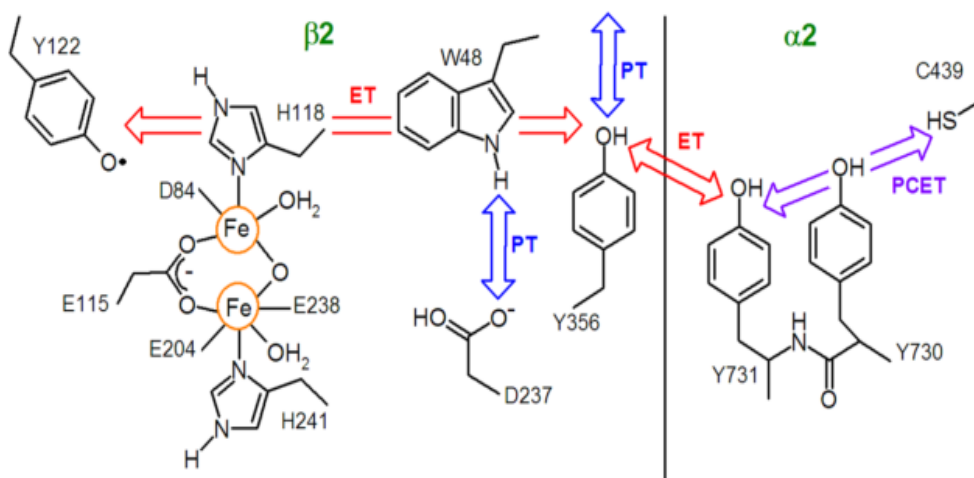


Figure 1.6. Putative long-range PCET pathway for catalysis in class Ia RNR. Note that there is no direct evidence for the role of W48.

1.2.2. Unnatural amino acids

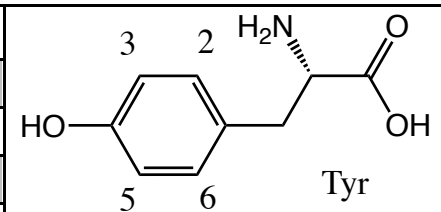
Unnatural amino acids (UAA) have extended the function of natural amino acids and provide mechanistic insight into protein function. Technologies such as intein chemistry and evolved aminoacyl-tRNA synthetase (aaRS) using amber suppressor tRNA have made it possible to selectively replace canonical residues with unnatural amino acids. This is an operation that is

reminiscent of site-specific mutagenesis.³¹⁻³³ Although their uses are quite diverse, these unnatural amino acids have played a particularly insightful role in the mechanistic study of PCET reactions in biological catalysis.

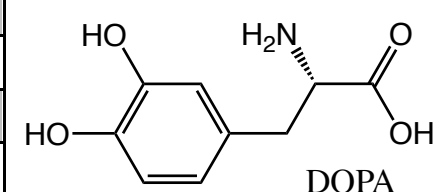
1.2.3. Unnatural tyrosine

A series of studies led by Prof. JoAnne Stubbe focused on changing the rate-limiting conformational control of the PCET process, in RNR preceding catalysis, towards PCET by site-selectively substituting the natural tyrosine residues implicated in the pathway for a series of unnatural tyrosine derivatives.^{23,34,35} Among the examples explored, fluorinated tyrosines (F_nY) and dihydroxyphenylalanine (DOPA) have emerged as two analogs for tyrosine sidechains with altered pK_a and/or reduction potentials (**Table 1.2**), that lead to either altered PCET rates or to uncoupled electron transfer (*i.e.* no proton transfer) upon insertion into the protein environment.^{24,27,36,37}

UAA	pK_a	E_p (V)	ΔE_p vs Y/Y• (mV)
Y	10	0.83	---
DOPA	9.7	0.57	-260
3-F-Y	8.4	0.77	-60
3,5-F ₂ Y	7.2	0.77	-60
2,3-F ₂ Y	7.8	0.86	30
2,3,5-F ₃ Y	6.4	0.86	30
2,3,6-F ₃ Y	7	0.93	100
2,3,5,6-F ₄ Y	5.6	0.97	140



Tyr



DOPA

Table 1.2. Peak potentials (E_p) and pK_a s of tyrosine UAAs and structure of F_n -tyrosine and 3,4-dihydroxyphenylalanine (DOPA).

1.2.4. Unnatural tryptophan

Tryptophanyl radicals formed via PCET are increasingly observed in proteins such as cryptochrome, cytochrome c peroxidase, DNA photolyase, and azurin. The functional role of tryptophanyl radicals in catalysis is directly related to systems such as cytochrome c oxidase and RNR,³⁸ however there is no direct evidence that tryptophanyl residues are involved in these

catalytically linked PCET reactions. The limitation of detection is often due to the transient nature of the tryptophanyl radical. This limitation can be addressed by altering the local thermodynamics that can be achieved by using unnatural amino acids. Prof. Schultz and Prof. Arnold report several unnatural tryptophan residues that focus on the development of tRNA synthetase / tRNA pairs (aaRS) using these tRNA pairs, tryptophan unnatural amino acids can be encoded in *E. coli* (**Figure 1.7**).^{39,40} Of these UAAs, there is either no activity (1,2) or no greatly altered reduction potential (3-5). Fluorotryptophan derivatives have received the most attention due to their selective ¹⁹F NMR active nuclei. Direct mono-fluorination of the indole ring modestly increases the ionization potential.³⁶ Further site-selective uptake of fluorotryptophan has not been achieved using the evolved aaRS strategy. Therefore, there is a shortage of functionally translatable tryptophan unnatural amino acids for PCET studies.

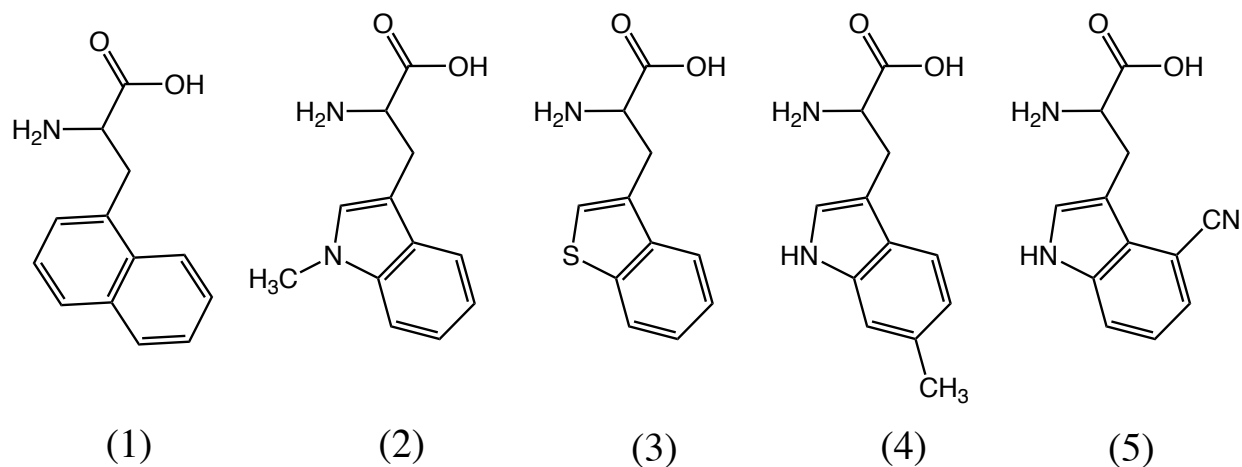
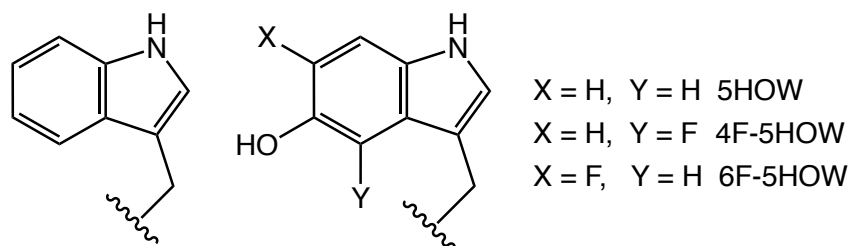


Figure 1.7. Available of UAAs of tryptophanyl residues^{39,40}

Tryptophan has a reduction potential of almost 100 mV higher than tyrosine at pH 7.²⁷ To provide a strategy for altering the tryptophan redox potential, 5-hydroxytryptophan (5HOW), which has been shown to have a reduced potential relative to tryptophan oxidation will be used in this thesis.^{41,42} As shown in the unnatural tyrosine study, halogenation of 5-HOW is expected to significantly reduce the pK_a of hydroxy group and change the spectral properties of the F_n-radical state. In fact, F_nYs have been utilized extensively in RNR to study PCET for these reasons. Thus, halogenated 5-hydroxytryptophans (5-HOWs) residues are expected to act as radical traps for

transiently oxidized tryptophan, thereby shifting the rate-limiting step(s) to radical transfer enabling the evaluation of the participation of tryptophan sidechains in long-range PCET in proteins. This thesis focuses on synthesis of a series of 5-HOWs (**Figure 1.8**) and uses fluorine to investigate their effects on pKa. Fluorine atoms are also expected to provide a unique spectroscopic reporter of tryptophanyl radicals.

Figure 1.8. Structures of tryptophan and F_n-5-HOW derivatives



1.2.5. Marcus Theory for Electron Transfer

Marcus electron transfer theory states that the electron transfer rate constant depends on the Gibbs free energy for the reaction, ΔG° , and on λ , the energy required to reorganize the nuclear configuration from that of the reactants to products.⁴³ The treatment is based on activated complex theory and simple harmonic potentials. The key parameters can be summarized in a plot of free energy versus reaction coordinate. Two overlapping parabolas represent potential energy surfaces for the reactants in the initial state and products in the final, electron transferred state. These parabolas represent the position where electron is in the reactant or product. Changes in driving force, ΔG° (the free energy difference between reactants and products) cause vertical displacements of the parabolas; changes in λ cause horizontal displacements. Larger horizontal displacements (larger values of λ) produce larger activation barriers. At constant λ , increases in driving force increase and then decrease the rate, generating the known inverted region. The maximum rate occurs when the absolute value of the driving force equals λ (**Figure 1.9**).^{29,38}

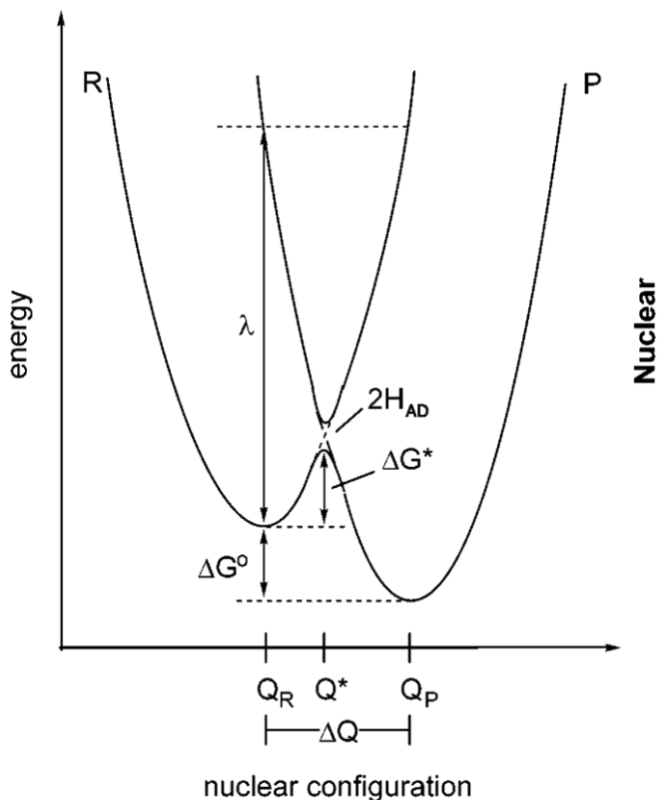


Figure 1.9. A simple energy scheme of the Marcus theory. The harmonic potential energy of the reactants and products as a function of the nuclear configuration for an electron transfer reaction. The variables are as follows λ is the reorganization energy, ΔG° is the driving force of the ET reaction, ΔG^* is the activation energy and H_{AD} is the electronic coupling.²⁹

How is this relevant to change in reduction potentials (E°) caused by UAAs? The relationship of driving force and reduction potential is from the relationship with Gibbs free energy and the Nernst equation (Equation 1.1). Unnatural amino acids exhibit altered reduction potentials, leading to significant changes to the driving force energy, ΔG° . These unnatural amino acids can thereby serve as thermodynamic traps for ET reactions, enabling a probe of ET, PT processes.

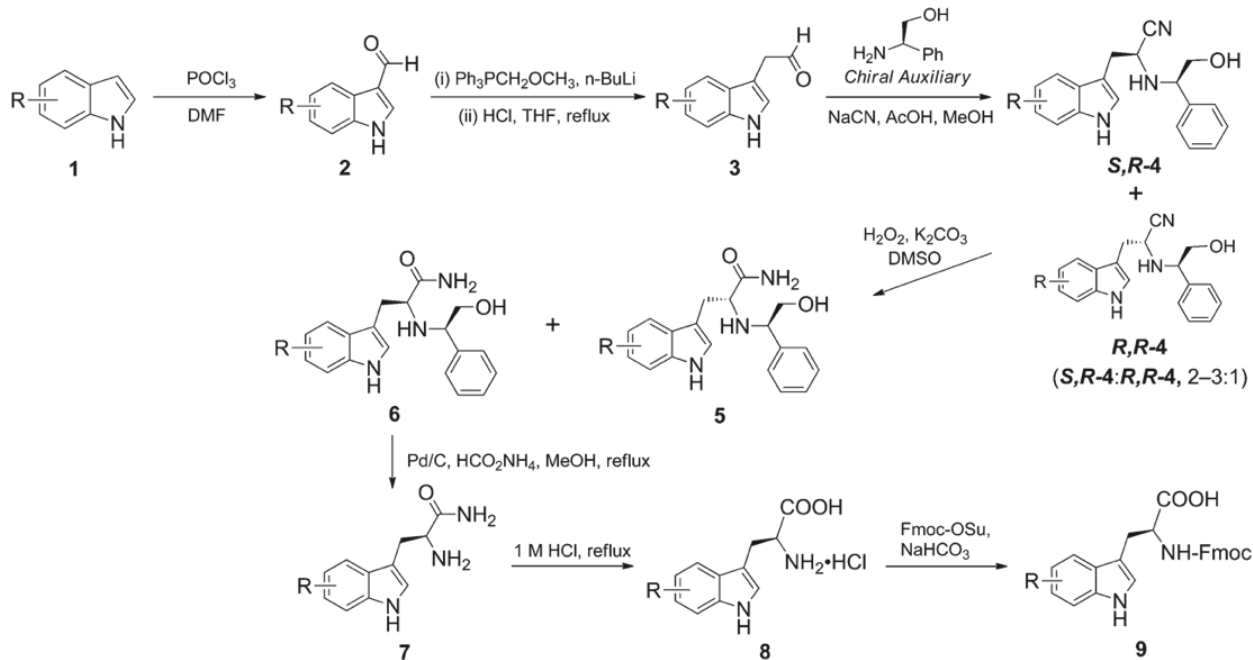
$$\Delta G = \Delta G^\circ + RT \ln Q$$

$$\Delta G^\circ = -nFE^\circ$$

Equation 1.1. Relationship of driving force ΔG° and reduction potentials E°

1.2.6. Conventional synthesis of hydroxy-L-tryptophan

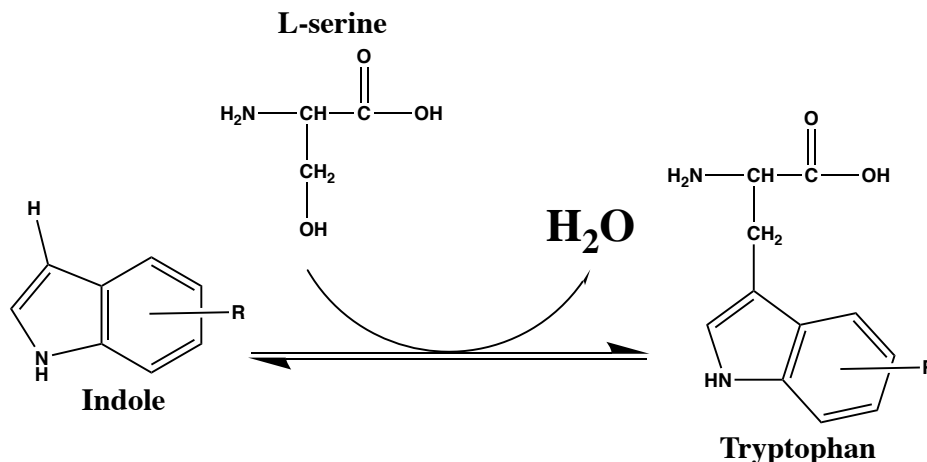
Unnatural amino acids are often not commercially accessible. While L-5-hydroxy tryptophan is commercially available, fluoro-5-hydroxy-L-tryptophans are not. However, organic synthesis of unnatural tryptophan sidechains with enantiomerically pure backbone is complicated and leads to low yields. As described by Prof. Chou-Hsiung Chen who studied making derivatives of tryptophan which were subsequently used for the convergent synthesis of a potent antibacterial agent, argyrin A and its analogues, there are seven steps for total synthesis of tryptophan derivatives. Moreover, this synthesis route requires several days. The final yield was 1.6 % for tryptophan from indole.⁴⁴ Therefore, we aim for an alternative biosynthetic route to make tryptophan derivatives which requires non-organic solvents and ambient pressure.



Scheme 1.2. the synthesis of tryptophan analogues ⁴⁴

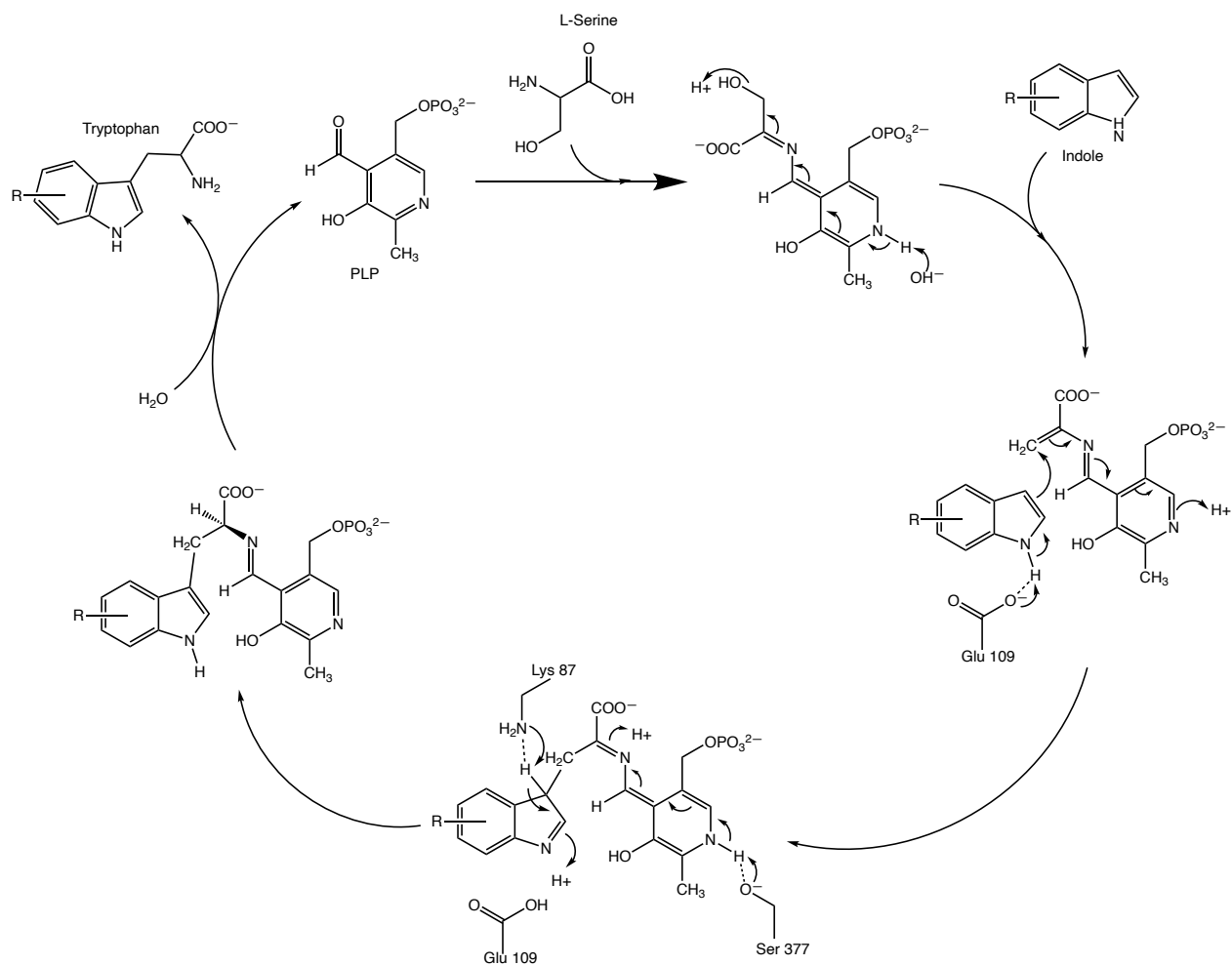
1.2.7. Mechanism and function of tryptophan B synthase: Altered synthetic route for unnatural tryptophans

Tryptophan synthase catalyzes the last two reactions in the biosynthesis of tryptophan. The bacterial enzyme consists of an $\alpha_2\beta_2$ tetramer in a linear α - β - β - α arrangement.⁴⁵ The β subunit catalyzes (TrpB) the condensation of indole with serine in a reaction mediated by pyridoxal phosphate (**Scheme 1.3** and **1.4**). The advantage of this biosynthesis process is that it is one step and only requires water as a solvent and ‘cheap’ L-serine as a starting material.⁴⁰



Scheme 1.3. synthesis of unnatural tryptophan from indole using Trp B synthase.

Naturally occurring TrpB is allosterically regulated by TrpA subunit and exhibits poor conversion of unnatural indole rings. A significant improvement of synthesis of unnatural tryptophan using TrpB synthase was reported by Prof. Arnold, whose lab applied directed evolution to generate a new, non-native variant of TrpB synthase, Tm9D8*, that has been shown to synthesize halogenated and 5-hydroxytryptophans (**Figure 1.10**) with yields up to 76 % at 37°C⁴⁰ (**Scheme 1.3** and **1.4**). This approach enables us to use TrpB as a means to make novel F_n-5HOWs from F_n-5HOIs.



Scheme 1.4. Mechanism of TrpB synthase conversion of indole to tryptophan using L-serine substrate and pyridoxal phosphate (PLP) cofactor.^{40,45}

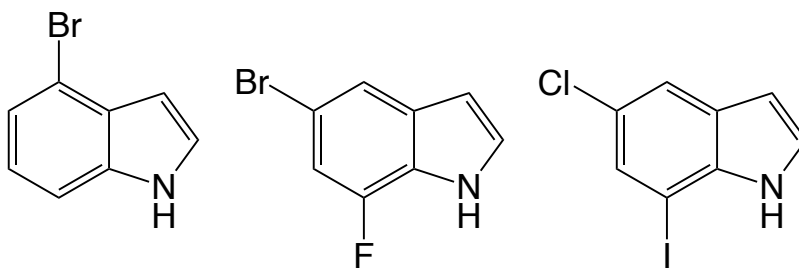
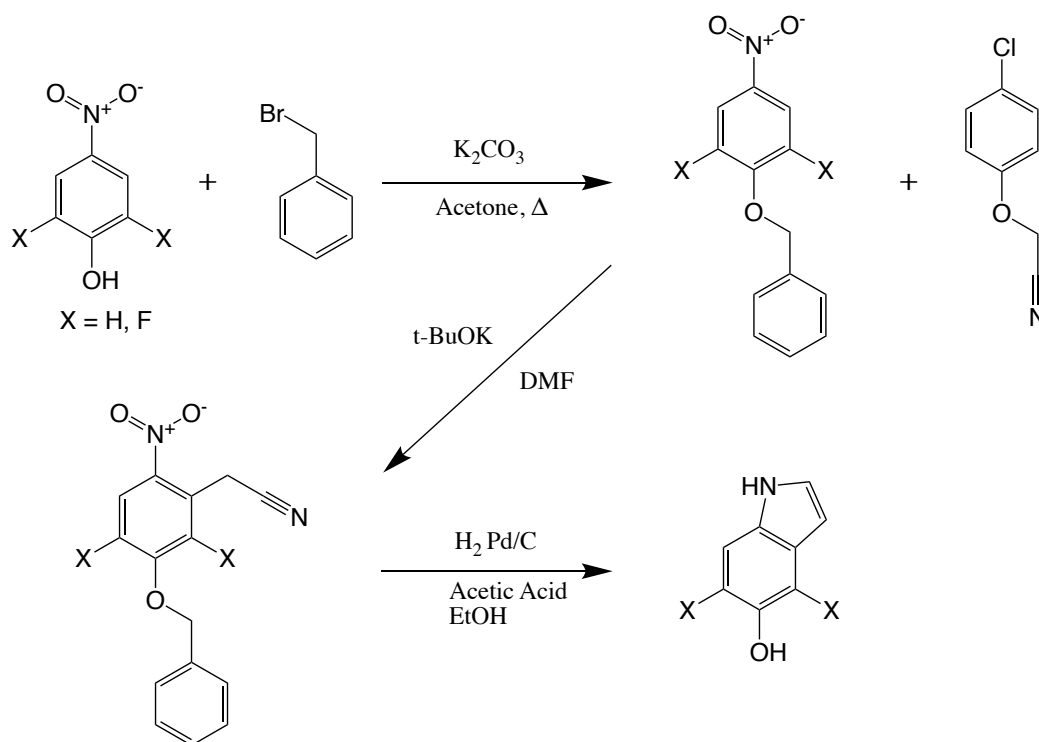


Figure 1.10. Examples of tested unnatural tryptophans backbone from Prof. Arnold.⁴⁰

1.2.8. Synthesis of unnatural indoles

Some of the unnatural indoles are commercially available however those can be expensive. Relevant to this thesis, 4F-5HOI and 6F-5HOI are not available commercially, we aimed to make it using organic synthesis as inspired by Prof Makosza.⁴⁶ They reported many ways to make indole derivatives which those are synthesized by nucleophilic substitution and hydrogenation (**Scheme 1.5**). They synthesized 5-methoxyindole and 5-hydroxyindole with around 80% yields. However, hydroxy group is reacted by nucleophilic reaction. Therefore, protection of hydroxy group is reacted in first steps and deprotection for hydroxy group is happens at the same time as hydrogenation.⁴⁷



Scheme 1.5. Synthesis of unnatural 5-hydroxyindole ^{46,47}

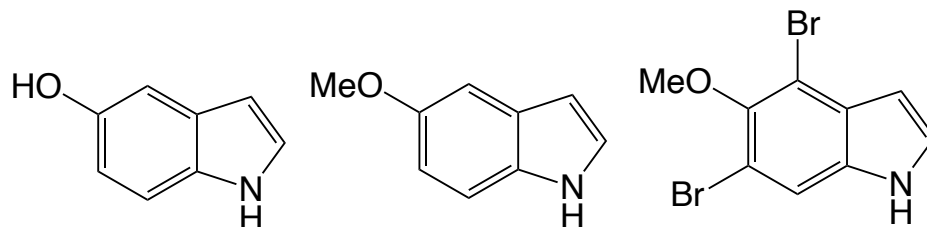


Figure 1.11. Synthesized indole products from Prof. Makosza. ^{46,48}

1.2.9. β -hairpin peptides to probe intermolecular forces.

In beta-hairpin structure, residues from across the strand are introduced that can influence the properties of amino acids cross strand. The force acting across the strand is called the intermolecular force. The peptide for this thesis was inspired by Prof. Waters who studies cation- π interaction in β -hairpin.⁴⁹ There are three types of intermolecular forces in the β -hairpin model peptide. First is van der Waals interaction that is distance dependent interaction between atoms or molecules; an example is 5-hydroxytryptophan and phenylalanine with π - π interaction in this unnatural peptide. Second is cation- π interaction that is a noncovalent intermolecular interaction that acts between an electron-rich π -electron system (hydroxytryptophan) and a neighboring cation ($^+\text{NH}_3$ group in lysine). And third is H-bond interaction that a hydrogen bond is a special type of dipole-dipole attraction which occurs when a hydrogen atom bonded to a strongly electronegative atom exists in the vicinity of another electronegative atom with a lone pair of electrons. Water solvent interacts with hydroxy and amine groups of 5-hydroxytryptophan, for example. Note that compared to the Waters peptide (**Figure 1.12**), 5-hydroxytryptophan was substituted for tryptophan, phenylalanine for leucine, and lysine for X in Prof. Water's peptide model (**Figure 1.12**). Those interactions are expected to affect the spectroscopic and redox properties which is pKa and electrochemical potentials.

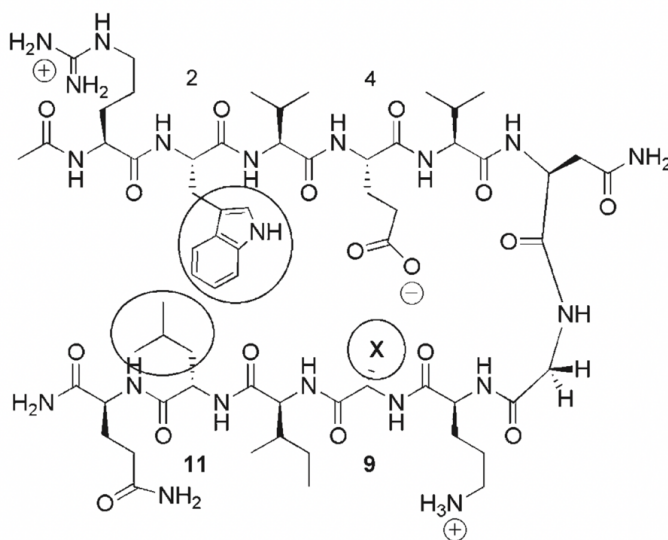


Figure 1.12. β -hairpin peptide model containing tryptophan⁴⁹

1.3. Thesis outline

Chapter 2 describes the synthesis of three new substrate mimics to test large volume substrates activity for double mutant soybean lipoxygenase towards novel hydroperoxide formation from biocatalytic C-H activation. The activation of C-H bonds is a key chemical transformation, representing a challenge in the design of asymmetric organometallic catalysts to generate a range of organic molecules with diverse functional groups. Soybean lipoxygenase-1 is a model enzyme that catalyzes C-H activation reactions.

Chapter 3 describes the synthesis of unnatural tryptophan amino acids using biosynthesis and model beta-hairpin peptide using solid peptide chemistry. Unnatural tryptophans were incorporated in a protein to study long-range proton coupled electron transfer pathways. The synthesis of unnatural difluorinated 5-hydroxyindole was attempted however, it was not synthesized well.

Appendix 1 describes the synthesis of oleyl sulfate as an allosteric effector for lipoxygenases

1.4. References

1. Offenbacher AR, Zhu H, Klinman JP. Synthesis of site-specifically ¹³C labeled linoleic acids. *Tetrahedron letters*. 2016;57(41):4537-4540. <http://dx.doi.org/10.1016/j.tetlet.2016.08.071>. doi: 10.1016/j.tetlet.2016.08.071.
2. Newton CG, Kossler D, Cramer N. Asymmetric catalysis powered by chiral cyclopentadienyl ligands. *Journal of the American Chemical Society*. 2016;138(12):3935-3941. <http://dx.doi.org/10.1021/jacs.5b12964>. doi: 10.1021/jacs.5b12964.
3. Hartwig JF. Catalyst-controlled site-selective bond activation. *Accounts of chemical research*. 2017;50(3):549-555. <http://dx.doi.org/10.1021/acs.accounts.6b00546>. doi: 10.1021/acs.accounts.6b00546.
4. Zhang Z, Tanaka K, Yu J. Remote site-selective C–H activation directed by a catalytic bifunctional template. *Nature (London)*. 2017;543(7646):538-542. <https://search.datacite.org/works/10.1038/nature21418>. doi: 10.1038/nature21418.
5. Chen G, Gong W, Zhuang Z, et al. Ligand-accelerated enantioselective methylene C(sp³)–H bond activation. *Science (American Association for the Advancement of Science)*. 2016;353(6303):1023-1027. <https://search.datacite.org/works/10.1126/science.aaf4434>. doi: 10.1126/science.aaf4434.
6. Zheng J, Wang S, Zheng C, You S. Asymmetric dearomatization of naphthols via a rh-catalyzed C(sp²)–H functionalization/annulation reaction. *Journal of the American Chemical Society*. 1900;137(15):4880-4883. <http://dx.doi.org/10.1021/jacs.5b01707>. doi: 10.1021/jacs.5b01707.
7. Lee JY, Karlin KD. Elaboration of copper–oxygen mediated C–H activation chemistry in consideration of future fuel and feedstock generation. *Current opinion in chemical biology*. 2015;25:184-193. <https://search.datacite.org/works/10.1016/j.cbpa.2015.02.014>. doi: 10.1016/j.cbpa.2015.02.014.
8. Oloo WN, Que L. Bioinspired nonheme iron catalysts for C–H and C–C bond oxidation: Insights into the nature of the metal-based oxidants. *Accounts of chemical research*. 2015;48(9):2612-2621. <http://dx.doi.org/10.1021/acs.accounts.5b00053>. doi: 10.1021/acs.accounts.5b00053.

9. Nanda S, Yadav JS. Lipoxygenase biocatalysis: A survey of asymmetric oxygenation. *Journal of molecular catalysis. B, Enzymatic*. 2003;26(1-2):3-28. [https://search.datacite.org/works/10.1016/s1381-1177\(03\)00146-2](https://search.datacite.org/works/10.1016/s1381-1177(03)00146-2). doi: 10.1016/s1381-1177(03)00146-2.
10. Porta H, Rocha-Sosa M. Plant lipoxygenases. physiological and molecular features. *Plant physiology (Bethesda)*. 2002;130(1):15-21. <https://search.datacite.org/works/10.1104/pp.010787>. doi: 10.1104/pp.010787.
11. Knapp MJ, Seebeck FP, Klinman JP. Steric control of oxygenation regiochemistry in soybean lipoxygenase-1. *Journal of the American Chemical Society*. 2001;123(12):2931-2932. <http://dx.doi.org/10.1021/ja003855k>. doi: 10.1021/ja003855k.
12. Cichewicz RH, Kenyon VA, Whitman S, et al. Redox inactivation of human 15-lipoxygenase by marine-derived meroditerpenes and synthetic chromanes: Archetypes for a unique class of selective and recyclable inhibitors. *Journal of the American Chemical Society*. 2004;126(45):14910-14920. <http://dx.doi.org/10.1021/ja046082z>. doi: 10.1021/ja046082z.
13. Knapp MJ, Rickert K, Klinman JP. Temperature-dependent isotope effects in soybean lipoxygenase-1: Correlating hydrogen tunneling with protein dynamics. *Journal of the American Chemical Society*. 2002;124(15):3865-3874. <http://dx.doi.org/10.1021/ja012205t>. doi: 10.1021/ja012205t.
14. Scheller G, Jager E, Hoffmann B, Schmitt M, Schreier P. Soybean lipoxygenase: Substrate structure and product selectivity. *Journal of the American Chemical Society*. 1995;43(7):1768-1774. <https://pubs.acs.org/doi/abs/10.1021/jf00055a005>. doi: 10.1021/jf00055a005.
15. Clapp CH, Pachuski J, Bassett NF, et al. N-linoleoylamino acids as chiral probes of substrate binding by soybean lipoxygenase-1. *Bioorganic chemistry*. 2018;78:170-177. <https://search.datacite.org/works/10.1016/j.bioorg.2018.03.010>. doi: 10.1016/j.bioorg.2018.03.010.
16. Arrigo Scettri, Francesco Bonadies, Alessandra Lattanzi, Laura Palombi, Silvia Pesci. Chemical, photochemical and enzymatic approach to furylhydroperoxides. *Tetrahedron*. 1997;53(50):17139-17150. [https://doi.org/10.1016/S0040-4020\(97\)10135-1](https://doi.org/10.1016/S0040-4020(97)10135-1). doi: 10.1016/S0040-4020(97)10135-1.

17. E. J. Corey, Nagata R. Evidence in favor of an organoiron-mediated pathway for lipoxygenation of fatty acids by soybean. *Journal of the American Chemical Society*. 1987;109:8207-8108. <https://pubs.acs.org/doi/pdfplus/10.1021/ja00260a038>. doi: 10.1021/ja00260a038.
18. Hu S, Offenbacher AR, Thompson EM, et al. Biophysical characterization of a disabled double mutant of soybean lipoxygenase: The “Undoing” of precise substrate positioning relative to metal cofactor and an identified dynamical network. *Journal of the American Chemical Society*. 2019;141(4):1555-1567. <http://dx.doi.org/10.1021/jacs.8b10992>. doi: 10.1021/jacs.8b10992.
19. Horitani M, Offenbacher AR, Carr CAM, et al. ¹³C ENDOR spectroscopy of Lipoxygenase–Substrate complexes reveals the structural basis for C–H activation by tunneling. *Journal of the American Chemical Society*. 2017;139(5):1984-1997. <https://search.datacite.org/works/10.1021/jacs.6b11856>. doi: 10.1021/jacs.6b11856.
20. Hu S, Sharma SC, Scouras AD, et al. Extremely elevated room-temperature kinetic isotope effects quantify the critical role of barrier width in enzymatic C-H activation. *Journal of the American Chemical Society*. 2014;136(23):8157-8860.
21. Gagliardi CJ, Westlake BC, Kent CA, Paul JJ, Papanikolas JM, Meyer TJ. Integrating proton coupled electron transfer (PCET) and excited states. *Coordination Chemistry Reviews*. 2010;254(21):2459-2471. <http://dx.doi.org/10.1016/j.ccr.2010.03.001>. doi: 10.1016/j.ccr.2010.03.001.
22. Torrents E. Ribonucleotide reductases: Essential enzymes for bacterial life. *Frontiers in cellular and infection microbiology*. 2014;4:52. <https://www.ncbi.nlm.nih.gov/pubmed/24809024>. doi: 10.3389/fcimb.2014.00052/full.
23. Seyedsayamdost MR, Yee CS, Reece SY, Nocera DG, Stubbe J. pH rate profiles of F_nY356-R₂s (n = 2, 3, 4) in escherichia coli ribonucleotide reductase: Evidence that Y356 is a redox-active amino acid along the radical propagation pathway. *Journal of the American Chemical Society*. 2006;128(5):1562. <https://www.ncbi.nlm.nih.gov/pubmed/16448127>.
24. Minnihan EC, Nocera DG, Stubbe J. Reversible, long-range radical transfer in E. coli class Ia ribonucleotide reductase. *Accounts of Chemical Research*. 2013;46(11):2524-2535. <http://dx.doi.org/10.1021/ar4000407>. doi: 10.1021/ar4000407.

25. Kolberg M, Strand KR, Graff P, Kristoffer Andersson K. Structure, function, and mechanism of ribonucleotide reductases. *BBA - Proteins and Proteomics*. 2004;1699(1):1-34. <http://dx.doi.org/10.1016/j.bbapap.2004.02.007>. doi: 10.1016/j.bbapap.2004.02.007.
26. Seyedsayamdost MR, Xie J, Chan CTY, Schultz PG, Stubbe J. Site-specific insertion of 3-aminotyrosine into subunit $\alpha 2$ of E. coli ribonucleotide reductase: Direct evidence for involvement of Y730 and Y731 in radical propagation. *Journal of the American Chemical Society*. 2007;129(48):15060-15071. <http://dx.doi.org/10.1021/ja076043y>. doi: 10.1021/ja076043y.
27. Seyedsayamdost MR, Reece SY, Nocera DG, Stubbe J. Mono-, di-, tri-, and tetra-substituted fluorotyrosines: New probes for enzymes that use tyrosyl radicals in catalysis. *Journal of the American Chemical Society*. 2006;128(5):1569-1579. <http://dx.doi.org/10.1021/ja055926r>. doi: 10.1021/ja055926r.
28. Siegbahn PEM, Eriksson L, Himo F, Pavlov M. Hydrogen atom transfer in ribonucleotide reductase (RNR). *The Journal of Physical Chemistry B*. 1998;102(51):10622-10629. <http://dx.doi.org/10.1021/jp9827835>. doi: 10.1021/jp9827835.
29. Stubbe J, Nocera DG, Yee CS, Chang MCY. Radical initiation in the class I ribonucleotide reductase: Long-range proton-coupled electron transfer? *Chemical Reviews*. 2003;103(6):2167-2202. <http://dx.doi.org/10.1021/cr020421u>. doi: 10.1021/cr020421u.
30. Kang G, Taguchi AT, Stubbe J, Drennan CL. Structure of a trapped radical transfer pathway within a ribonucleotide reductase holocomplex. *Science (American Association for the Advancement of Science)*. 2020;368(6489):424-427. <https://www.ncbi.nlm.nih.gov/pubmed/32217749>. doi: 10.1126/science.aba6794.
31. Dougherty DA. Unnatural amino acids as probes of protein structure and function. *Current Opinion in Chemical Biology*. 2000;4(6):645-652. [http://dx.doi.org/10.1016/S1367-5931\(00\)00148-4](http://dx.doi.org/10.1016/S1367-5931(00)00148-4). doi: 10.1016/S1367-5931(00)00148-4.
32. Young TS, Ahmad I, Yin JA, Schultz PG. An enhanced system for unnatural amino acid mutagenesis in E. coli. *Journal of molecular biology*. 2010;395(2):361-374. <https://search.datacite.org/works/10.1016/j.jmb.2009.10.030>. doi: 10.1016/j.jmb.2009.10.030.

33. Noren C, Anthony-Cahill S, Griffith M, Schultz P. A general method for site-specific incorporation of unnatural amino acids into proteins. *Science (American Association for the Advancement of Science)*. 1989;244(4901):182-188.
<https://search.datacite.org/works/10.1126/science.2649980>. doi: 10.1126/science.2649980.
34. Ravichandran KR, Taguchi AT, Wei Y, Tommos C, Nocera DG, Stubbe J. A >200 meV uphill thermodynamic landscape for radical transport in escherichia coli ribonucleotide reductase determined using fluorotyrosine-substituted enzymes. *Journal of the American Chemical Society*. 2016;138(41):13706-13716. <https://www.ncbi.nlm.nih.gov/pubmed/28068088>. doi: 10.1021/jacs.6b08200.
35. Yokoyama K, Smith AA, Corzilius B, Griffin RG, Stubbe J. Equilibration of tyrosyl radicals (Y356•, Y731•, Y730•) in the radical propagation pathway of the E. coli class ia ribonucleotide reductase. *Journal of the American Chemical Society*. 2011;133(45):18420-18432.
https://www.openaire.eu/search/publication?articleId=od_____267::d34b2ea95fabac0b0ec85fd44b20fcbc. doi: 10.1021/ja207455k.
36. Minnihan EC, Young DD, Schultz PG, Stubbe J. Incorporation of fluorotyrosines into ribonucleotide reductase using an evolved, polyspecific aminoacyl-tRNA synthetase. *Journal of the American Chemical Society*. 2011;133(40):15942-15945.
<http://dx.doi.org/10.1021/ja207719f>. doi: 10.1021/ja207719f.
37. Offenbacher AR, Vassiliev IR, Seyedsayamdost MR, Stubbe J, Barry BA. Redox-linked structural changes in ribonucleotide reductase. *Journal of the American Chemical Society*. 2009;131(22):7496-7497. <http://dx.doi.org/10.1021/ja901908j>. doi: 10.1021/ja901908j.
38. Migliore A, Polizzi NF, Therien MJ, Beratan DN. Biochemistry and theory of proton-coupled electron transfer. *Chemical Reviews*. 2014;114(7):3381-3465.
<http://dx.doi.org/10.1021/cr4006654>. doi: 10.1021/cr4006654.
39. Chatterjee A, Xiao H, Yang P, Soundararajan G, Schultz PG. A tryptophanyl-tRNA synthetase/tRNA pair for unnatural amino acid mutagenesis in E. coli. *Angewandte Chemie (International ed.)*. 2013;52(19):5106-5109.
<https://search.datacite.org/works/10.1002/anie.201301094>. doi: 10.1002/anie.201301094.
40. Boville CE, Romney DK, Almhjell PJ, Sieben M, Arnold FH. Improved synthesis of 4-Cyanotryptophan and other tryptophan analogues in aqueous solvent using variants of TrpB

- from *thermotoga maritima*. *Journal of organic chemistry*. 2018;83(14):7447-7452.
<http://dx.doi.org/10.1021/acs.joc.8b00517>. doi: 10.1021/acs.joc.8b00517.
41. Anthony Harriman. Further comments on the redox potentials of tryptophan and tyrosine. *Journal of the American Chemical Society*. 1987.
<https://pubs.acs.org/doi/pdf/10.1021/j100308a011>. doi: 10.1021/j100308a011.
42. Barry BA. Proton coupled electron transfer and redox active tyrosines in photosystem II. *Journal of Photochemistry & Photobiology, B: Biology*. 2011;104(1):60-71.
<http://dx.doi.org/10.1016/j.jphotobiol.2011.01.026>. doi: 10.1016/j.jphotobiol.2011.01.026.
43. Marcus RA. Electron transfer reactions in chemistry. theory and experiment. *Reviews of modern physics*. 1993;65(3):599-610.
<https://search.datacite.org/works/10.1103/revmodphys.65.599>. doi: 10.1103/revmodphys.65.599.
44. Chen C, Genapathy S, Fischer PM, Chan WC. A facile approach to tryptophan derivatives for the total synthesis of argyrian analogues. *Org Biomol Chem*. 2014;12(48):9764-9768.
<http://dx.doi.org/10.1039/C4OB02107J>. doi: 10.1039/C4OB02107J.
45. Karen S. Anderson, Edith W. Miles II, Kenneth A. Johnson. Serine modulates substrate channeling in tryptophan synthase. *THE JOURNAL OF BIOLOGICAL CHEMISTRY*. 1991;266(13):8020-8033.
46. Małkosza M, Danikiewicz W, Wojciechowski K. Reactions of organic anions, 147. simple and general synthesis of hydroxy- and methoxyindoles via vicarious nucleophilic substitution of hydrogen. *Liebigs Annalen der Chemie*. 1988;1988(3):203-208.
<https://onlinelibrary.wiley.com/doi/abs/10.1002/jlac.198819880304>. doi: 10.1002/jlac.198819880304.
47. Simon E. Kolstoe, Palma P. Mangione, Vittorio Bellotti, et al. Trapping of palindromic ligands within native transthyretin prevents amyloid formation. *Proceedings of the National Academy of Sciences - PNAS*. 2010;107(47):20483-20488.
<https://www.jstor.org/stable/25756723>. doi: 10.1073/pnas.1008255107.
48. Małkosza M, Wojciechowski K. Application of nucleophilic substitution of hydrogen in nitroarenes to the chemistry of indoles. *Chem Heterocycl Comp*. 2015;51(3):210-222.
<https://search.datacite.org/works/10.1007/s10593-015-1687-4>. doi: 10.1007/s10593-015-1687-4.

49. Hughes R, Benshoff M, Waters M. Effects of chain length and N-methylation on a cation- π interaction in a β -hairpin peptide. *Chemistry : a European journal*. 2007;13(20):5753-5764. <https://search.datacite.org/works/10.1002/chem.200601753>. doi: 10.1002/chem.200601753.

Chapter 2

Design of unnatural, lipoxygenase-targeted substrates towards novel hydroperoxide formation from biocatalytic C-H activation

2.1. Strategy

This chapter describes the synthesis of three new substrate mimics (**1-3**) to test large volume substrates activity for double mutant soybean lipoxygenase. Synthesis of **1** (**Figure 2.1**) proceed through a Cu(I)-assisted Grignard coupling reaction of **5**, generated from 3,4-dihydro-2*H*-pyran protection (DHP) of commercially available 9-decyn-1-ol **4**, with commercially available benzyl bromide (**Scheme 2.1**). Upon generation of the coupled **6**, the desired final product, **1**, is achieved through the sequence of deprotection (*p*-toluene sulfonic acid in dry methanol), alcohol oxidation (Jones oxidation catalyst, **Figure 2.1**), and alkyne reduction (Lindlar catalyst, H₂, **Scheme 2.1**). Synthesis of compound **2** and **3** proceeds in a comparable manner as **1**, except for the substitution of benzyl bromide with the commercially available starting materials, cyclopropyl acetylene for compound **2** after brominating compound **5**. While compound **1** represents structural mimics of linoleic acid with carbons C1-C13 remaining the same with substitution of C14-C18 to a volume-filling group, compounds **2** and **3** structural mimics of linoleic acid with carbons C1-C11 remaining the same with substitution of C12-C18 to a volume-filling group. Yields for many steps are near quantitative except for the Cu(I)-assisted C-C bond formation step to form compound **6**, which typically results in ~ 50% yields after purification for LA.¹ As an alternative approach, Meyer and Klinman reported the use of 2 molar equivalents of CuI/NaI in anhydrous

DMF with slight excess of K_2CO_3 to couple the methyl ester of compound **4** with 1-bromo-2-octyne in high yields (~80%).²

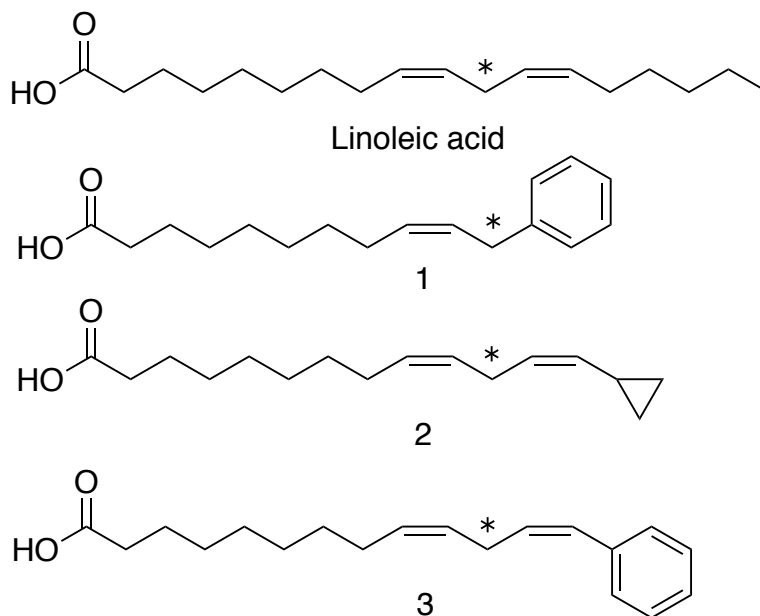


Figure 2.1. New designed of unnatural substrates for LOX. The anticipated reactive carbon is shown (*)

2.2. Synthesis of unnatural substrate

2-(dec-9-yn-1-yloxy)tetrahydro-2H-pyran (5) was successfully synthesized. To a 100 mL round bottom flask (RBF) with a 1" PTFE stir bar, 0.22 g of *p*-toluenesulfonic acid (1.62 mmol) was dissolved with stirring in 20 mL anhydrous dichloromethane. 3,4-dihydro-2H-pyran (DHP) was added to the solution (1.43 g; 17.02 mmol), which turned red. 2.5 g of 9-decyn-1-ol, **4**, (Spectrum Chemicals; 16.20 mmol) in 20 mL dichloromethane was added dropwise. The reaction proceeded overnight at room temperature. The solution was quenched with 30 mL saturated sodium bicarbonate solution, extracted with 3 x 20 mL hexanes, dried with magnesium sulfate, and filtered through a silica plug. Solvent was removed by low pressure. The desired product, confirmed by TLC (silica; 4:1 hexanes:ethyl acetate) and $KMnO_4$ stain, was purified by flash chromatography using 1000 mL 4:1 hexanes:ethyl acetate. Solvent was removed to yield a colorless oil (2.82 g; 11.83 mmol; 73% yield). 1H NMR (400 MHz, $CDCl_3$), δ = 4.59 (t, 1H), 3.88

(m, 1H), 3.73 (m, 1H), 3.53 (m, 1H), 3.41 (m, 1H), 2.19 (td, 2H), 1.95 (t, 1H), 1.84 (m, 1H), 1.72 (m, 1H), 1.56 (m, 8H), 1.34 (m, 8H).

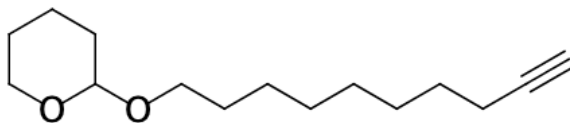


Figure 2.2. Structure of 2-(dec-9-yn-1-yloxy)tetrahydro-2H-pyran (**5**)

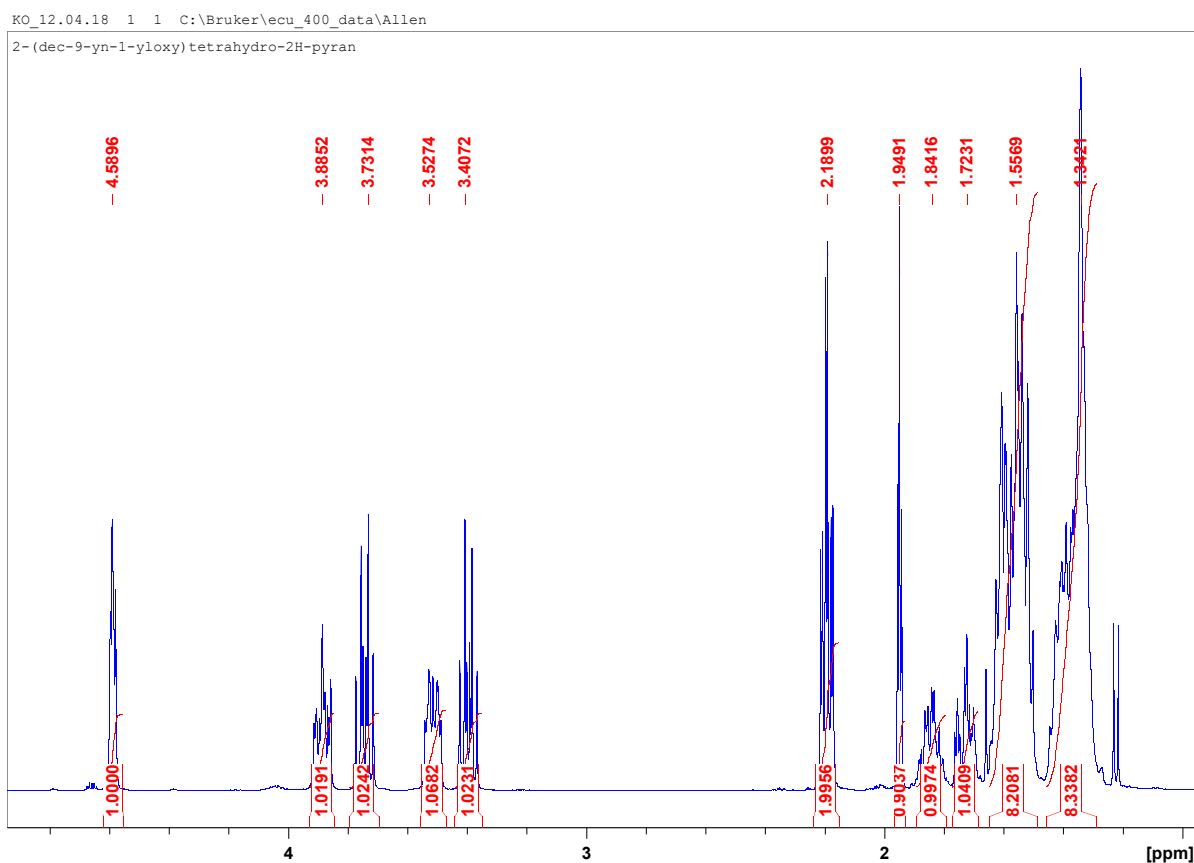
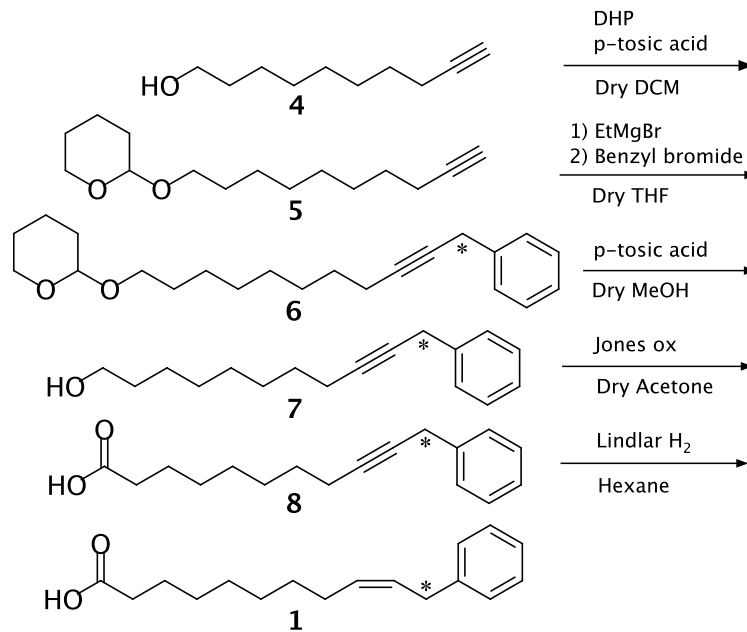


Figure 2.3. ^1H NMR spectrum of 2-(dec-9-yn-1-yloxy)tetrahydro-2H-pyran (**5**)

The first approach of 2-(11-phenylundec-9-ynyloxy)tetrahydro-2H-pyran (**6**) is using Grignard reagent in **scheme 2.1**.¹ In a dried and nitrogen purged 100mL of 3-neck flask with 1” PTFE stir bar and 0.7g of 2-(dec-9-yn-1-yloxy)tetrahydro-2H-pyran (**5**) (2.94mmol) was dissolved with stirring in 30mL of anhydrous THF. 3.91mL of 3M of ethyl magnesium bromide (11.75mmol) was transferred with closed shield wire tube into 3-neck flask. The reaction was carried out at 0°C for 1 hour and 0.02g of copper cyanide (0.25mmol) and 0.33mL of benzyl

bromide (3.23mmol) were added into solution. The reaction was carried out overnight with room temperature. The reaction was quenched with 20mL of saturate ammonium chloride, extracted with 20mL of hexane and 20mL of ethyl acetate 3 times, dried with magnesium sulfate, and filtered. The solvent was removed by low pressure. There was no spot in TLC plates with different concentration of hexane and ethyl acetate solvent.

The second approach of 2-(11-phenylundec-9-ynyloxy)tetrahydro-2H-pyran (6) is using sodium hydride instead of Grignard reagent. In a dried and nitrogen purged 100 mL 3-neck flask with 1" PTFE stir bar, 2-(dec-9-yn-1-yloxy)tetrahydro-2H-pyran (**5**) (0.2 g, 0.84 mmol), and sodium hydride (60%) after washed by hexane (0.05g 1.26 mmol) were added to 30 mL of THF that had been distilled over calcium hydride at 0°C for 10 minutes. To this, was added (1.02 g, 6.0 mmol) benzyl bromide. The reaction was allowed to stir at room temperature for overnight under nitrogen. The reaction was quenched with 100 mL of water and THF was removed by low pressure. Solution was extracted with 5 times of 30 mL dichloromethane. The collected organic layers were dried with anhydrous magnesium sulfate and filtered. The solvent was removed. The target product was not confirmed by TLC. There was no spot in TLC plates with different concentration of hexane and ethyl acetate solvent.



Scheme 2.1. Synthetic route pursued for **1**, inspired by the synthesis of linoleic acid

The alternative approach of 2-(11-phenylundec-9-ynoxy)tetrahydro-2H-pyran (**6**) is using copper iodide/sodium iodide, and potassium carbonate in anhydrous DMF for coupling reaction in **Scheme 2.2**. Before setting coupling reaction, starting product requires oxidation of alcohol to carboxylic acid and protection to ester. In 100 mL round bottom flask, 9-decyn-1-ol (1.0g, 6.48 mmol) was added to 50 mL of acetone. Jones reagent (2M) was added dropwise into acetone solution that color was changed to orange solution and mixed for 30 minutes. The reaction was poured into isopropanol that color of solution was changed to light blue. The solvent was removed by low pressure. Carboxyl group with 9-decyn-1-ol was added to 20 mL of anhydrous methanol and 5 drops of sulfuric acid and mixed for 5 minutes. The reaction was poured into a solution made by 50 mL of saturated potassium carbonate solution and filtered to separate and solution. The solvent was removed by low pressure. The reaction was poured into 25mL of dichloromethane and 25 mL water and extracted with five 25 mL portions of dichloromethane. The collected organic layers were dried with anhydrous magnesium sulfate and filtered. The solvent was removed and purified using flash chromatography in a 12" X 2" column of silica 60 with 90 % hexanes / 10% ethyl acetate. Solvent was removed to yield a light brown oil (0.8 g; 4.38

mmol; 67.7% yield). ^1H NMR (400 MHz, CDCl_3), δ = 3.68 (s, 3H), 2.32 (t, 2H), 2.20 (m, 2H), 1.95 (m, 1H), 1.56 (m, 4H), 1.34 (m, 7H).

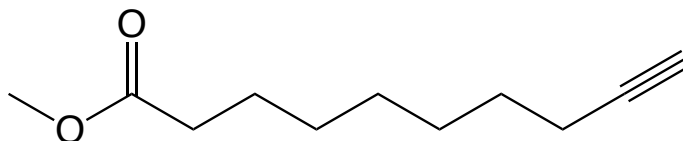


Figure 2.4. Structure of methyl dec-9-ynoate (**9**)

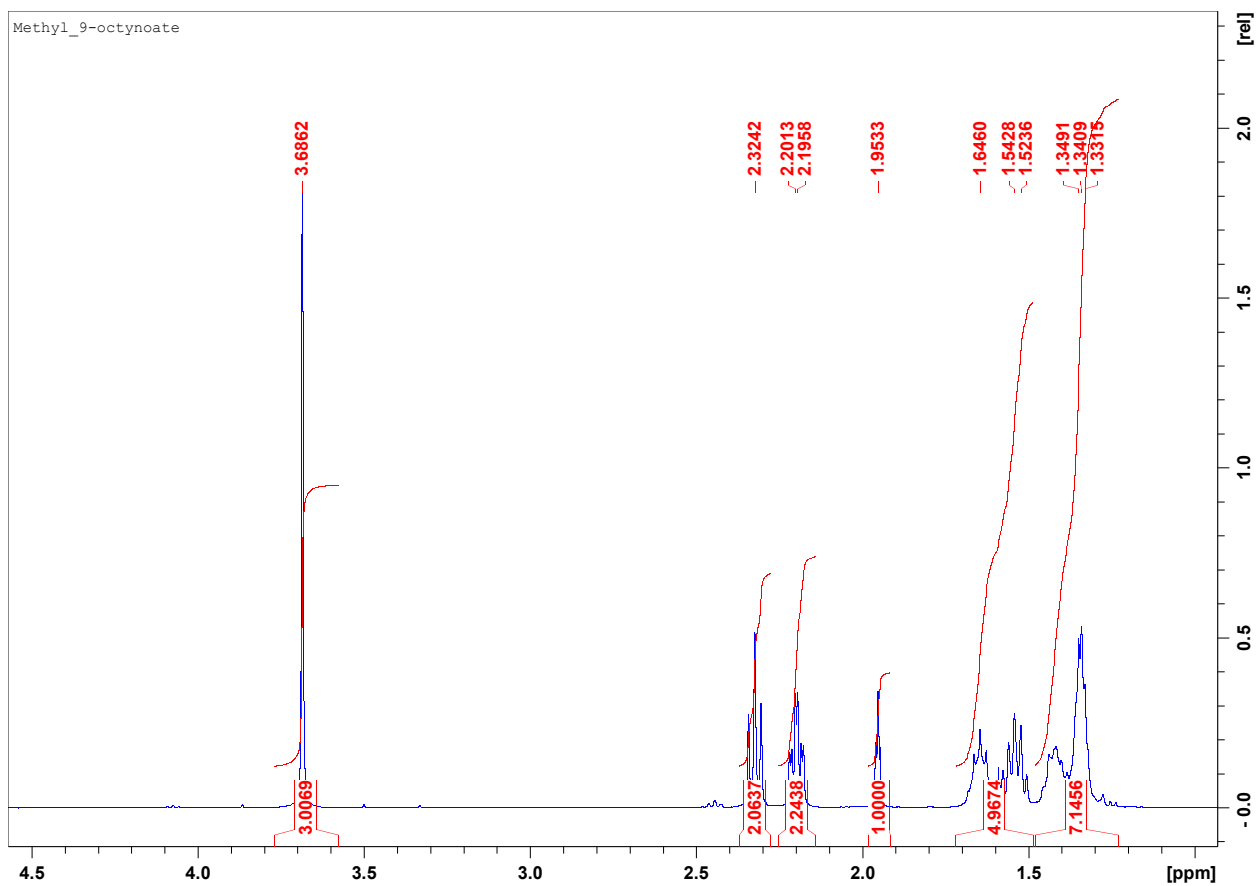


Figure 2.5. ^1H NMR of methyl dec-9-ynoate (**9**)

In a dried and nitrogen purged 100 mL round bottom flask, (2.27 g, 11.9 mmol) copper iodide, (1.79 g, 11.9 mmol) sodium iodide, and (1.23 g, 8.9 mmol) potassium carbonate were added to 30 mL of dimethylformamide (DMF) that had been distilled over calcium hydride. To this, was added (0.75 g, 4.1 mmol) of methyl dec-9-ynoate and then (1.02 g, 6.0 mmol) added benzyl bromide. The reaction was allowed to stir for 12 hours under nitrogen. The reaction was poured into a solution made by mixing 100 mL saturated ammonium chloride and 100 mL water and extracted with five 50 mL portions of diethyl ether. The collected organic layers were dried with anhydrous magnesium sulfate and filtered. The solvent was removed to give a combination of benzyl bromide and methyl 9,12-octadecadiynoate which was further purified using flash chromatography in a 12" X 2" column of silica 60 with 500 mL of 90 % hexanes / 10% ethyl acetate. The result of ^1H NMR showed benzyl bromide was not reacted with methyl dec-9-ynoate (9).

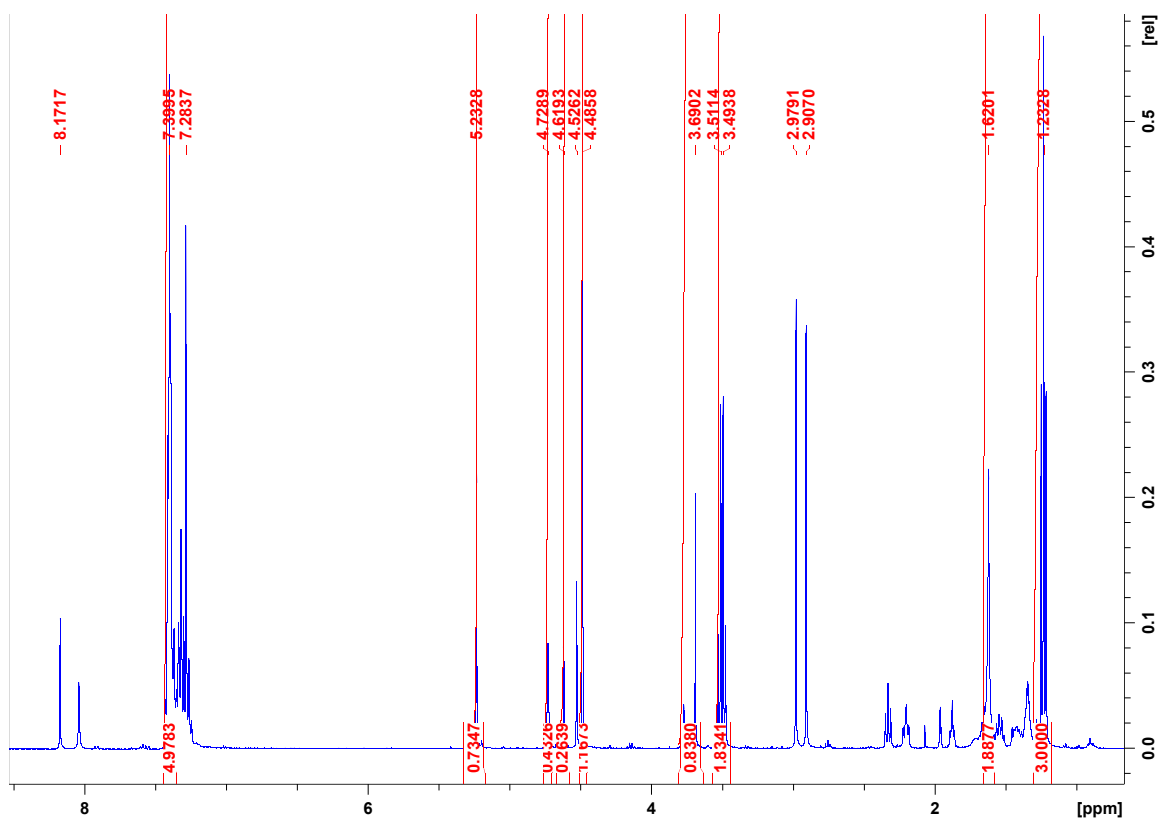
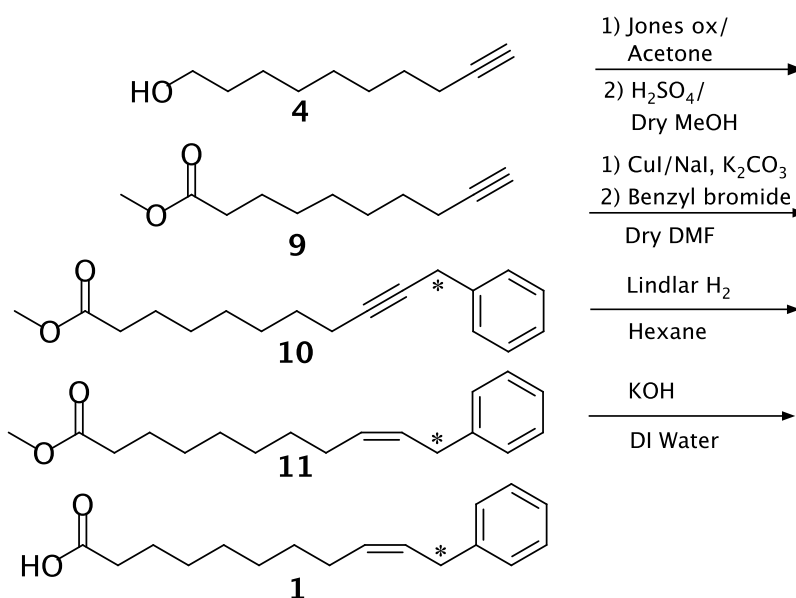


Figure 2.6. ^1H NMR of purified product of CuI/NaI reaction



Scheme 2.2. Alternative route pursued for synthesis of **1**.

2.3. Synthesis of different strategy of unnatural substrates

The synthesis of compound **2** (**Scheme 2.3**) is using Grignard reagent for making alcohol from compound **5** to compound **12**. In a dried and nitrogen purged 100 mL 3-neck round bottom flask, (3.13 g, 13.13 mmol) 2-(dec-9-yn-1-yloxy)tetrahydro-2H-pyran (**5**) and (0.949 g, 29.61 mmol) paraformaldehyde powder were added to 30 mL of anhydrous tetrahydrofuran that had been distilled over calcium hydride. To this, was added dropwise (10ml, 30.0 mmol) of 3M of ethyl magnesium bromide and reacted at around -10°C in 1 hour then heated up in room temperature for 2 hours. The reaction was allowed to stir for overnight under nitrogen. The reaction was poured into a solution made by mixing 100 mL saturated ammonium chloride and 100 mL water and extracted with three times of 25 mL portions of diethyl ether and three times 25 mL of hexane. The collected organic layers were dried with anhydrous magnesium sulfate and filtered. The solvent was removed to give a combination of paraformaldehyde and 11-(tetrahydro-2H-pyran-2-yloxy)undec-2-yn-1-ol (**12**) which was further purified using flash chromatography in a 12" X 2" column of silica 60 with 90 % hexanes / 10% diethyl ether. Solvent was removed to yield a colorless oil (2.74 g; 10.21 mmol; 77.7% yield). ¹H NMR (400 MHz, CDCl₃), δ = 4.59 (t, 1H),

4.26 (t, 2H), 3.88 (m, 1H), 3.73 (m, 1H), 3.50 (m, 1H), 3.41 (m, 1H), 2.22 (td, 2H), 1.84 (m, 1H), 1.72 (m, 1H), 1.56 (m, 8H), 1.34 (m, 8H).

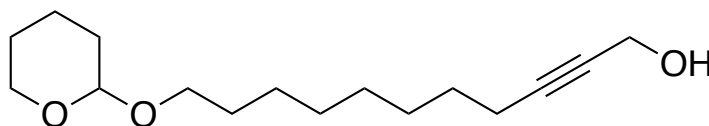


Figure 2.7. Structure of 11-(tetrahydro-2*H*-pyran-2-yloxy)undec-2-yn-1-ol (**12**)

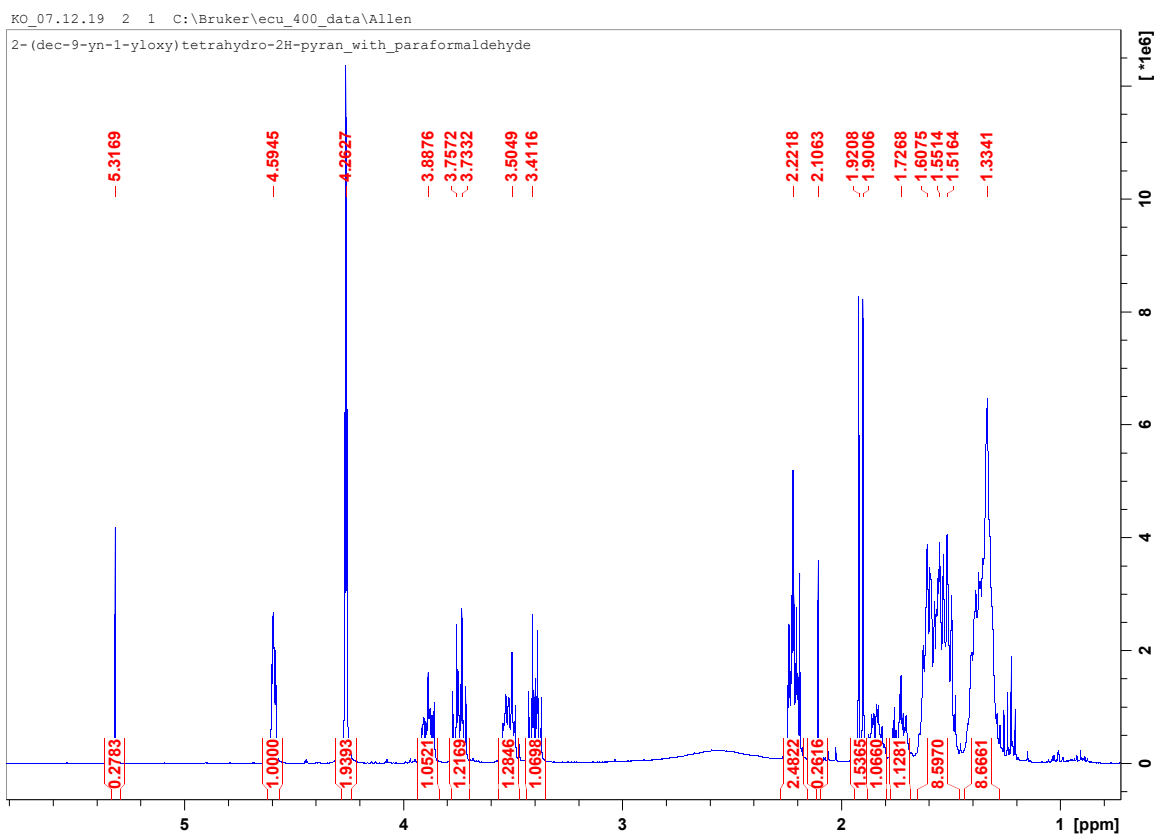


Figure 2.8. ^1H NMR spectrum of 11-(tetrahydro-2*H*-pyran-2-yloxy)undec-2-yn-1-ol (**12**)

2-(11-bromoundec-9-ynyloxy)tetrahydro-2*H*-pyran (**13**) was successfully synthesized. In a dried and nitrogen purged 100 mL of 3-neck round bottom flask, (4.02g, 15.21 mmol) triphenylphosphine was added to 30 mL of anhydrous dichloromethane at -10°C . To this, was added dropwise (0.78 mL, 15.31 mmol) bromine and 10 ml of dichloromethane and mixed 20 minutes at -10°C . (1.24 mL, 15.31 mmol) anhydrous pyridine was added to dichloromethane

solution and mixed 20 minutes at -10°C . Into 3-neck round flask, (2.74g, 10.21 mmol) 11-(tetrahydro-2*H*-pyran-2-yloxy)undec-2-yn-1-ol (**12**) dissolved with 10 mL of dichloromethane was added to triphenylphosphine and bromine solution for 2 hours at -10°C . The reaction was quenched with 100 mL of pentane for 30 minutes and filtered triphenylphosphine. The solvent was removed in low pressure. The compounds were extracted by 50 mL of pure water with three times of 25 mL of dichloromethane. The collected organic layers were dried with anhydrous sodium sulfate and filtered. The solvent was removed to give a combination of 2-(11-bromoundec-9-ynyloxy)tetrahydro-2*H*-pyran (**13**) which was purified using flash chromatography in a 12" X 2" column of silica 60 with 80 % dichloromethane / 20% ethyl acetate. Solvent was removed to yield a brown oil (2.17 g; 6.55 mmol; 64.2% yield). ^1H NMR (400 MHz, CDCl_3), δ = 4.59 (t, 1H), 3.95 (t, 2H), 3.88 (m, 1H), 3.73 (m, 1H), 3.50 (m, 1H), 3.41 (m, 1H), 2.25 (td, 2H), 1.84 (m, 1H), 1.72 (m, 1H), 1.56 (m, 8H), 1.34 (m, 6H).

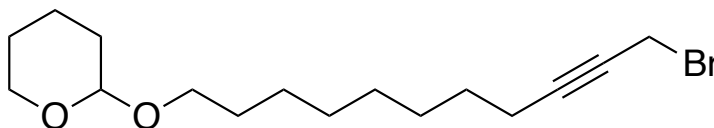


Figure 2.9. Structure of 2-(11-bromoundec-9-ynyloxy)tetrahydro-2*H*-pyran (**13**)

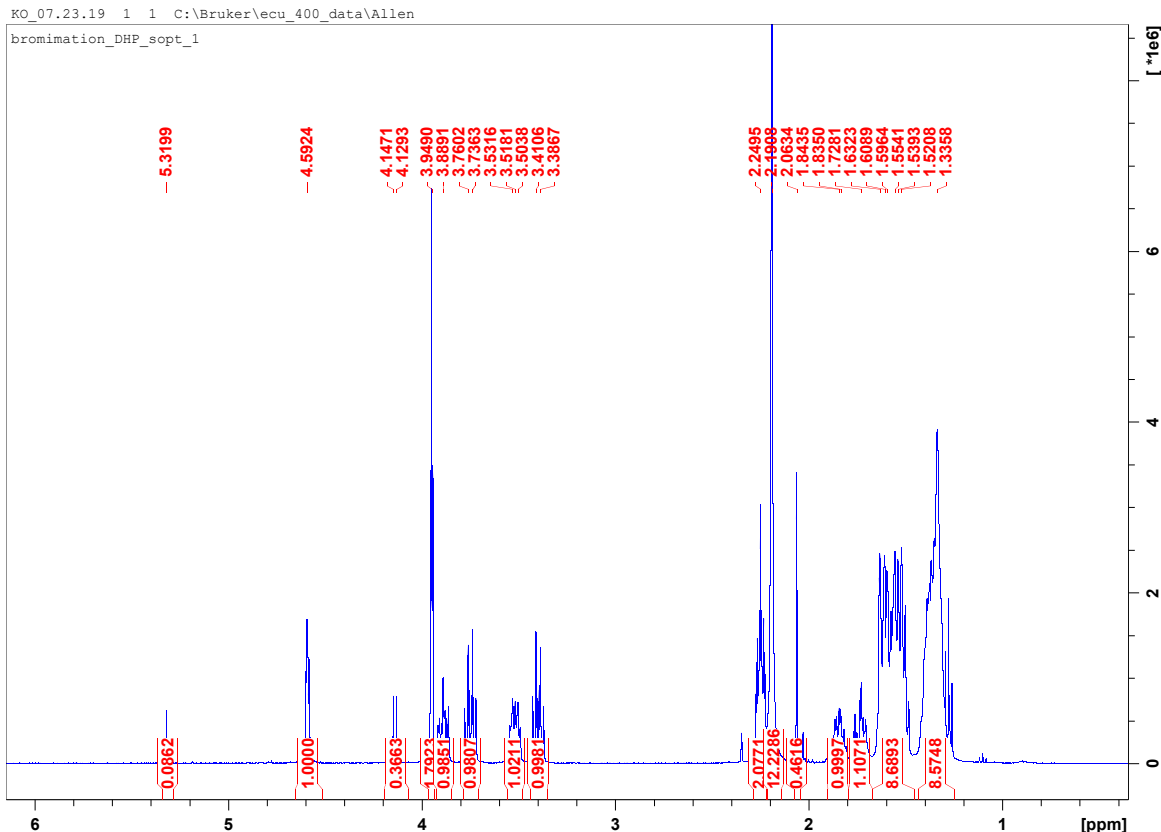
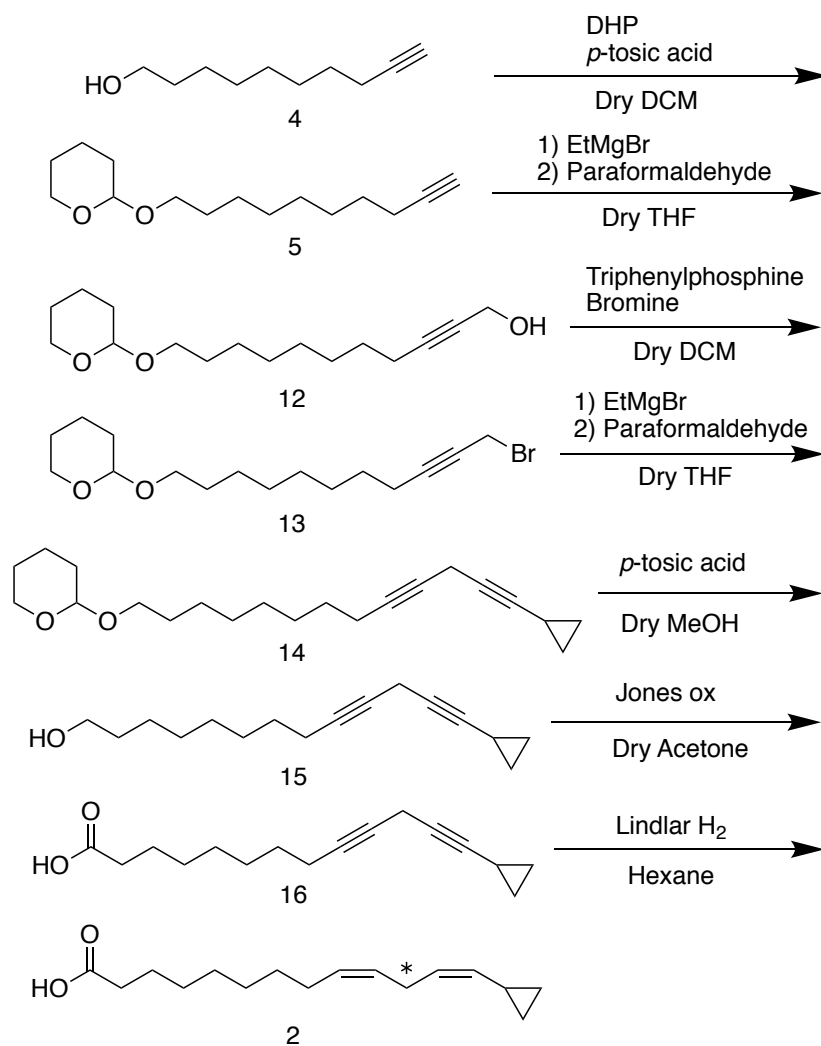


Figure 2.10. ^1H NMR spectrum of 2-(11-bromoundec-9-ynyloxy)tetrahydro-2*H*-pyran (**13**)

In a dried and nitrogen purged 100mL of 3-neck flask with 1" PTFE stir bar and 0.7g of 2-(11-bromoundec-9-ynyloxy)tetrahydro-2*H*-pyran (**13**) (0.3g, 0.91mmol) was dissolved with stirring in 30mL of anhydrous THF. 0.6mL of 3M of ethyl magnesium bromide (1.81mmol) was transferred with closed shield wire tube into 3-neck flask. The reaction was carried out at 0°C for 1 hour and 0.02g of copper cyanide (0.25mmol) and 0.15mL of cyclopropyl acetylene (1.81mmol) were added into solution. The reaction was carried out overnight with room temperature. The reaction was quenched with 20mL of saturate ammonium chloride, extracted with 20mL of hexane and 20mL of ethyl acetate 3 times, dried with magnesium sulfate, and filtered. The solvent was removed by low pressure. The product was not confirmed by TLC with potassium permanganate. There was no spot in TLC plates with different concentration of hexane and ethyl acetate solvent.



Scheme 2.3. New approach to making new set of unnatural substrates

2.4. Discussion

Products before the coupling reaction were success to get pure products by step by step however, any coupling reactions in these strategies were not successful. The reason Grignard coupling reaction was not successful is Grignard reagent is used for transformation into aldehyde or carboxylic acid not for alkyne. The other approaches for coupling reaction were using sodium hydride or copper iodide/sodium iodide instead of Grignard reagent for deprotonating proton at alkyne bond however, those approaches were not successful either. In 3rd strategy (**Scheme 2.3.**) is totally new approach for synthesizing for large volume substrate. The advantage of this approach

is that is not required for brominated compound for the other side of substrate chain and be able to use commercially available compound.

2.5. References

1. Offenbacher AR, Zhu H, Klinman JP. Synthesis of site-specifically ¹³C labeled linoleic acids. *Tetrahedron letters*. 2016;57(41):4537-4540. <http://dx.doi.org/10.1016/j.tetlet.2016.08.071>. doi: 10.1016/j.tetlet.2016.08.071.
2. Meyer MP, Klinman JP. Synthesis of linoleic acids combinatorially labeled at the vinylic positions as substrates for lipoxygenases. *Tetrahedron letters*. 2008;49(22):3600-3603. <http://dx.doi.org/10.1016/j.tetlet.2008.04.023>. doi: 10.1016/j.tetlet.2008.04.023.

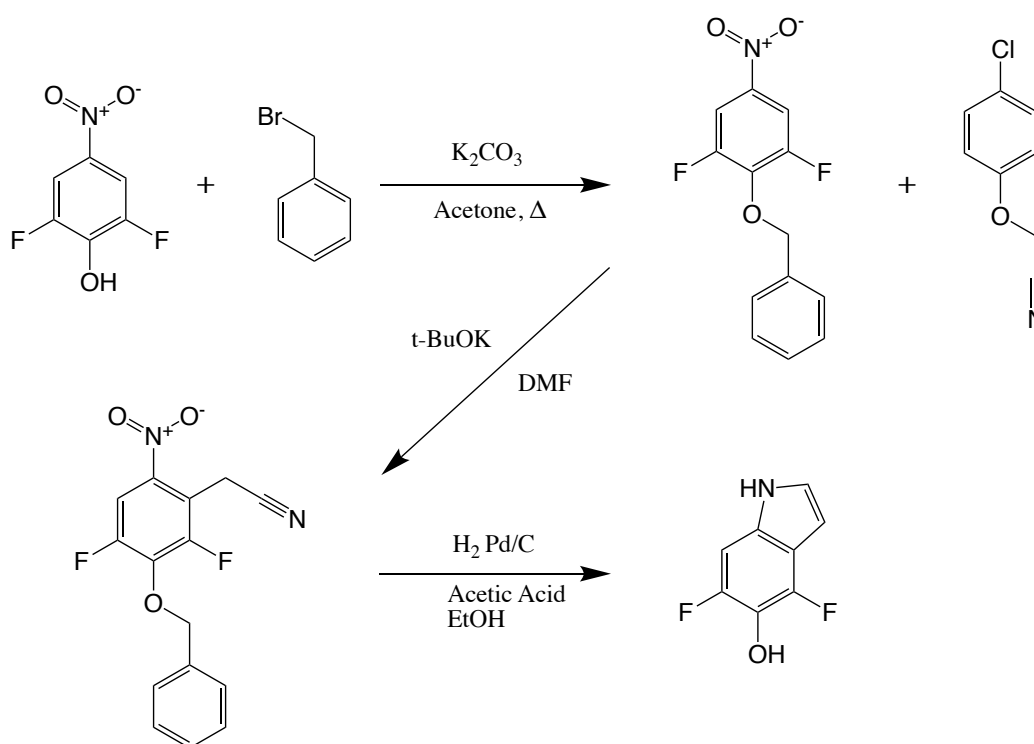
Chapter 3

Design of unnatural tryptophan amino acid to study proton coupled electron transfer

3.1. Synthesis of unnatural indoles.

The synthesis pathways were inspired by synthesis of mono fluorinated indole for 4,6-difluoro-5-hydroxy indole.^{1,2} Synthesis of difluoro hydroxy indole proceeds through a protection reaction for hydroxy group, coupling reaction, and hydrogenation with deprotection in same time.

(Scheme 3.1)



Scheme 3.1. Synthesis of 4,6-difluoro-5-hydroxy indole.

In protection reaction, to 100 mL round bottom flask with a 1 PTFE stir bar, 1g of 2,6-difluoro-4-nitrophenol (5.8mmol) and 2.7g of potassium carbonate (19.53mmol) were dissolved with stirring in 20 mL of acetone. 3.5mL of benzyl bromide (29.5mmol) was added into RBF. The reaction was carried out at 75°C for 24 hours. The solution was poured into 100 mL of cold water after RBF was cooled down for 40 minutes, extracted with 3 x 30 mL of dichloromethane, 20mL of brine solution, dried with magnesium sulfate, and filtered to separate salt solution. 50mL of

ammonium hydroxide was added into solution to mix for 30 minutes. The solution was extracted with 3 x 50 mL of DI water, 3 x 50 mL of 3M hydrochloric acid, dried with magnesium sulfate, and filtered. The solvent was removed by low pressure.

In coupling reaction, 2.16g of protected 2,6-difluoro-4-nitrophenol (12mmol) and 3.02g of 4-chlorophenoxy acetonitrile (18mmol) were dissolved in 20mL of anhydrous DMF in 250mL of 3-neck flask. 2.96g of potassium tert-butoxide with 20 mL of anhydrous DMF were into closed funnel which is attached on the 3-neck flask. Potassium tert-butoxide solution was added into 3-neck flask dropwise at -10°C for 3 hours after purging the air by nitrogen gas. The reaction was quenched into 250mL of 5% of HCl solution, extracted with 3 x 30 mL of dichloromethane and 3 x 30 mL of potassium carbonate, dried with magnesium sulfate, and filtered to separate salt and solution. The solvent was removed by low pressure and vacuum for recrystallizing. The desired product, confirmed by TLC (silica; 100% of dichloromethane), was purified by flash chromatography using 1000 mL of dichloromethanes. Solvent was removed to yield a light brown solid (2.39 g; 7.86 mmol; 65.5% yield).

In hydrogenation reaction, palladium on carbon (10% by mass of 10% by with Pd, 50 mg) was cautiously added to a deoxygenated stirring solution of 2,6-difluoro-3-methylcyanoide-4-nitrophenol (0.39 g, 1.3 mmol) in 10mL of acetic acid and 50mL of ethanol. The mixture was subjected to two cycles of evacuation and purging with hydrogen gas before being stirred under an atmosphere of hydrogen gas for 3 hours. The reaction was purged with air, filtered, solvent removed by low pressure, extracted with 3 x 30 mL of dichloromethane and 30 mL of sodium bicarbonate, dried with magnesium sulfate, and filtered to separate salt and solution. The solvent was rotovated off by low pressure. The product was not confirmed by TLC because of many plots in TLC plates with different concentration of dichloromethane and ethyl acetate solvent. 4,6-5HOI could not synthesized. Thus, 4F-5HOI and 6F-5HOI could be purchased from Enovations.

3.2. Synthesis of unnatural tryptophans with biosynthesis.

To a 250mL round bottom flask with a 1 PTFE stir bar, 0.27 g 5-hydroxyindole or 0.3 g F_n-hydroxyindole was dissolved in N₂-purged 100 mL of 20 mM potassium phosphate, pH 7.5,

supplemented with 18 mM (0.9 eq.) L-serine, 5-10 μ M Tm9D8* TrpB synthase. The RBF was closed and incubated at 37°C for 4 hours. TrpB synthase was removed by chelation with Ni-NTA beads. 0.6g of Sodium bicarbonate (4 eq.) and 1.21g of Fmoc-succinimide (2 eq.) were added with 100 mL 1,4-dioxane. The reaction was degassed and proceeded overnight with robust stirring at room temperature. The reaction RBF was then cooled to 0°C and the solution was acidified (pH 2-3) with HCl and filtered. Extraction was completed with ethyl acetate and the products were washed with a brine solution 3 times. The solution was dried with sodium sulfate and filtered into a round bottom flask. The solvent was removed by low pressure. The product was purified by reverse phase HPLC (40:60:0.1 to 80:20:0.1 acetonitrile:water:TFA). The HPLC solvent was removed by lyophilization.

Fmoc-5HOW: ^1H NMR (400 MHz, DMSO), δ = 12.65 (s, 1H), 10.53 (s, 1H), 8.57 (s, 1H), 7.87 (d, 2H), 7.65 (m, 2H), 7.0-7.4 (m, 7H), 6.86 (d, 1H), 6.61 (d, 1H), 4.19 (m, 3H), 2.96 (m, 2H). MS, observed: 441.83; predicted ($\text{C}_{26}\text{H}_{22}\text{N}_2\text{O}_5$): 442.15.

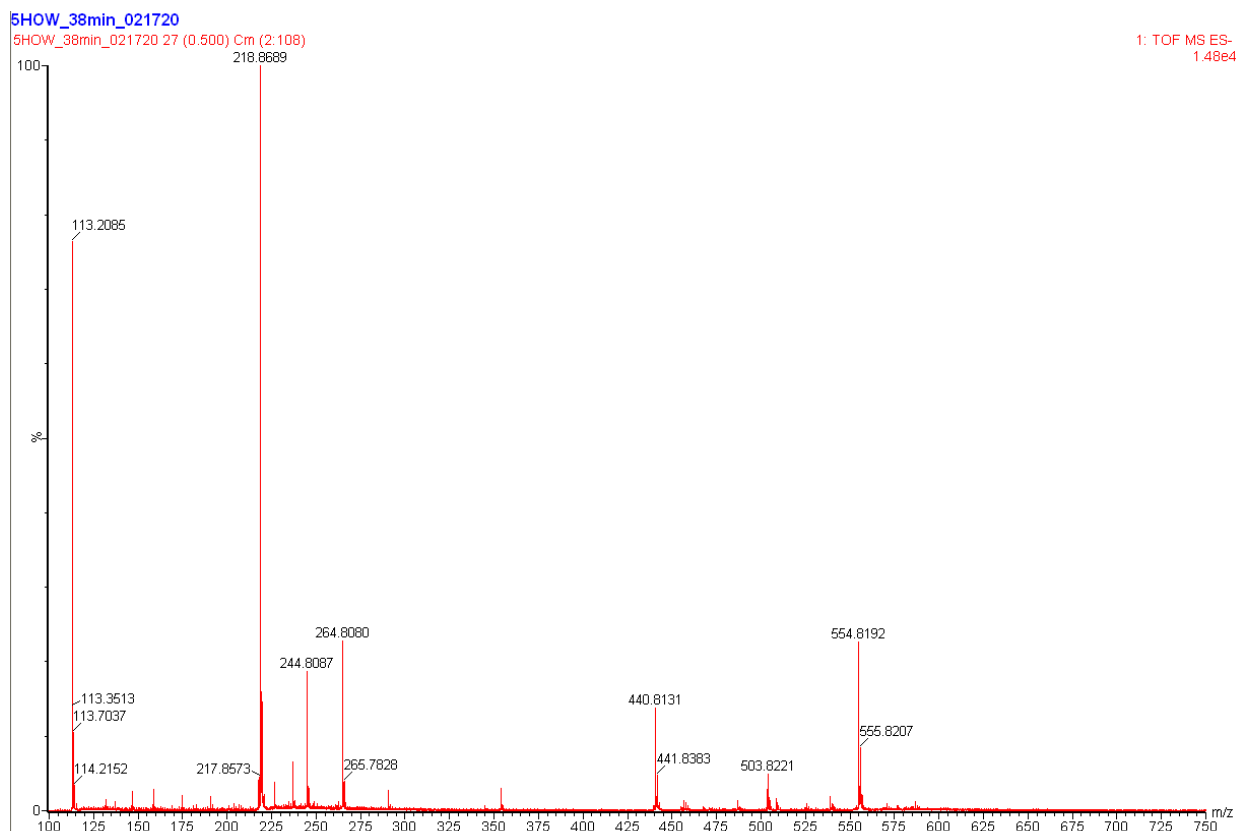


Figure 3.1. LC-MS result of Fmoc-5HOW

fmoc-5-HOW-02.17.20

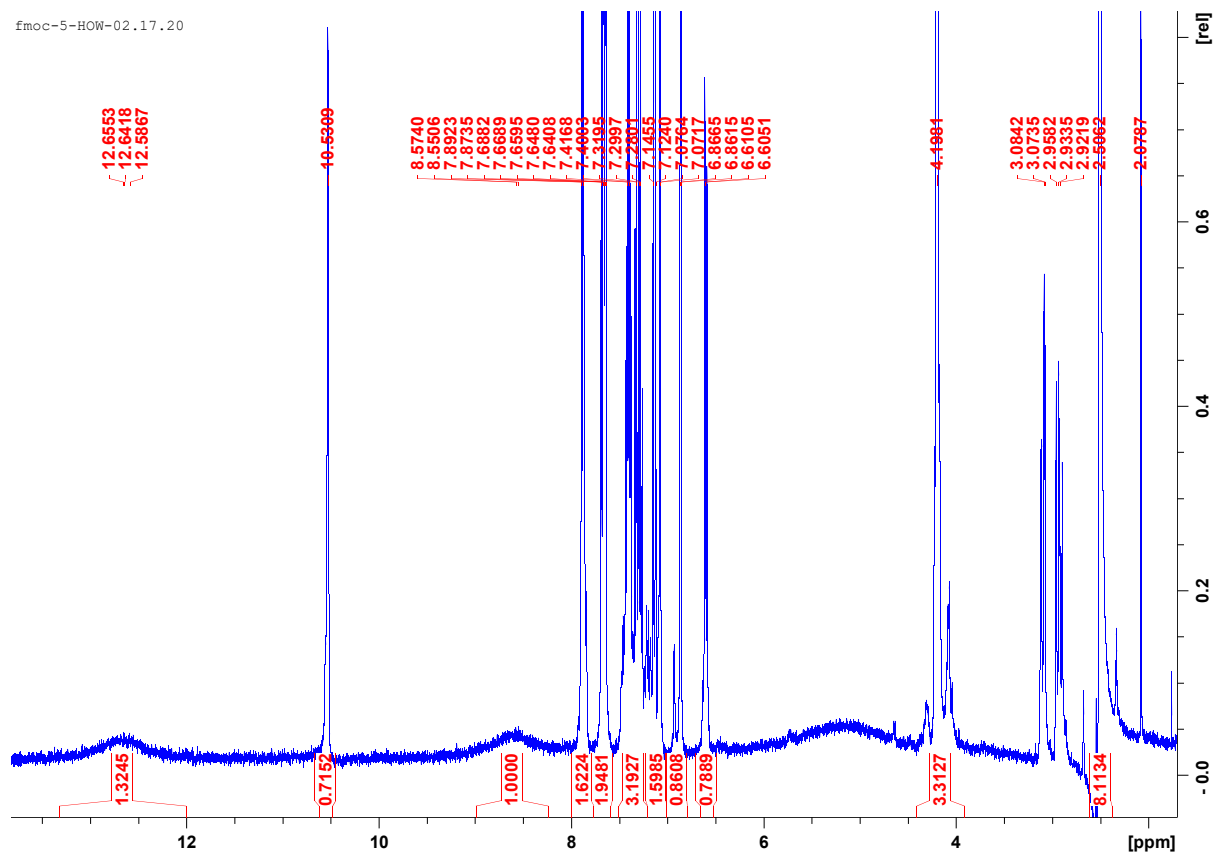


Figure 3.2. ¹H NMR spectra of fmoc-5HOW

Fmoc-4F-5HOW: ^1H NMR (400 MHz, DMSO), δ = 12.56 (s, 1H), 10.77 (s, 1H), 8.78 (s, 1H), 7.87 (d, 2H), 7.65 (m, 2H), 7.2-7.4 (m, 3H), 7.06 (s, 1H), 6.96 (d, 1H), 6.72 (s, 1H), 4.18 (m, 3H), 3.0-3.3 (m, 4H). ^{19}F NMR, -150.37 ppm. MS, observed: 459.43; predicted ($\text{C}_{26}\text{H}_{21}\text{FN}_2\text{O}_5$): 460.14.

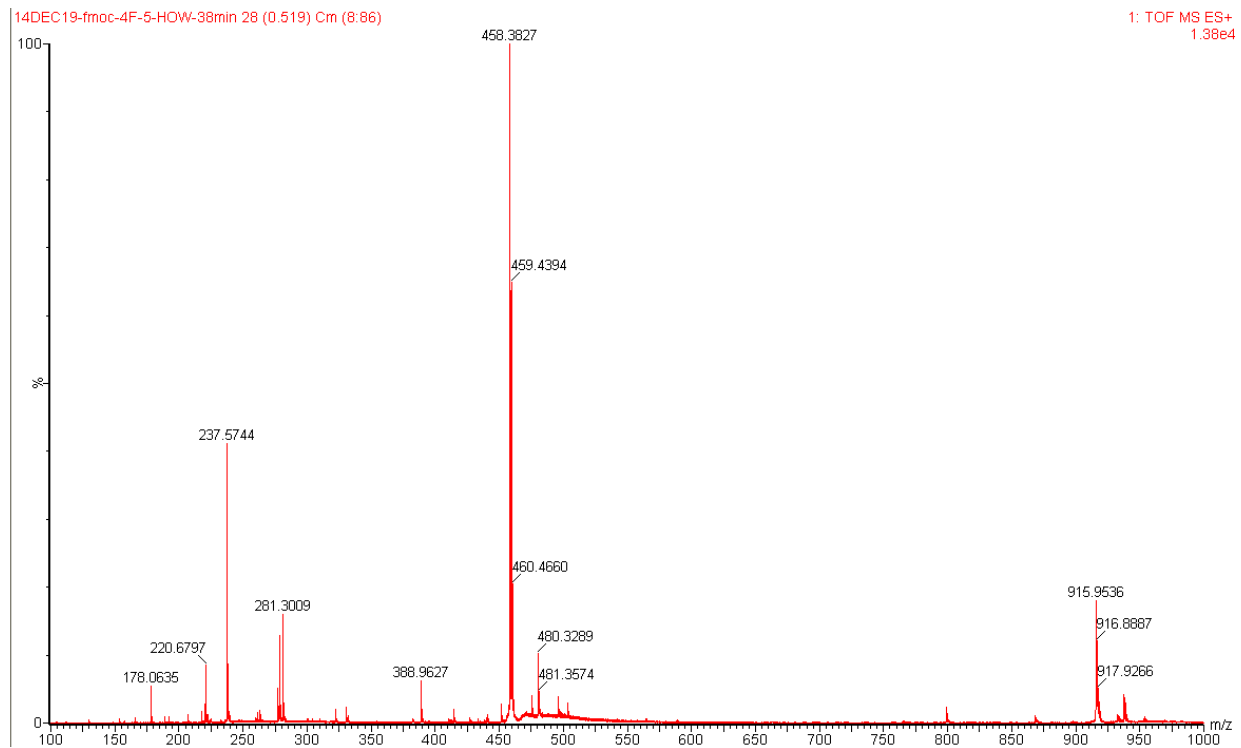


Figure 3.3. LC-MS result of fmoc-4F-5HOW

fmoc-4-F-5-HOW-12.05.19

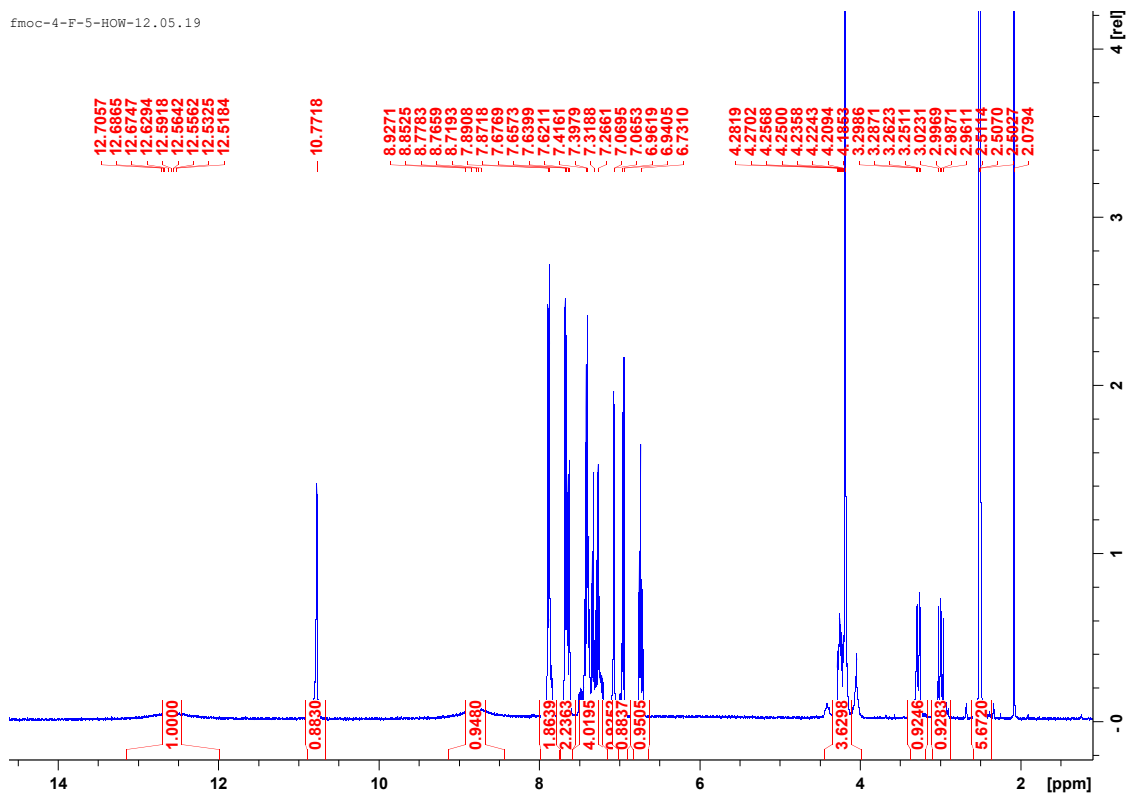


Figure 3.4. ¹H NMR spectra of fmoc-4F-5HOW

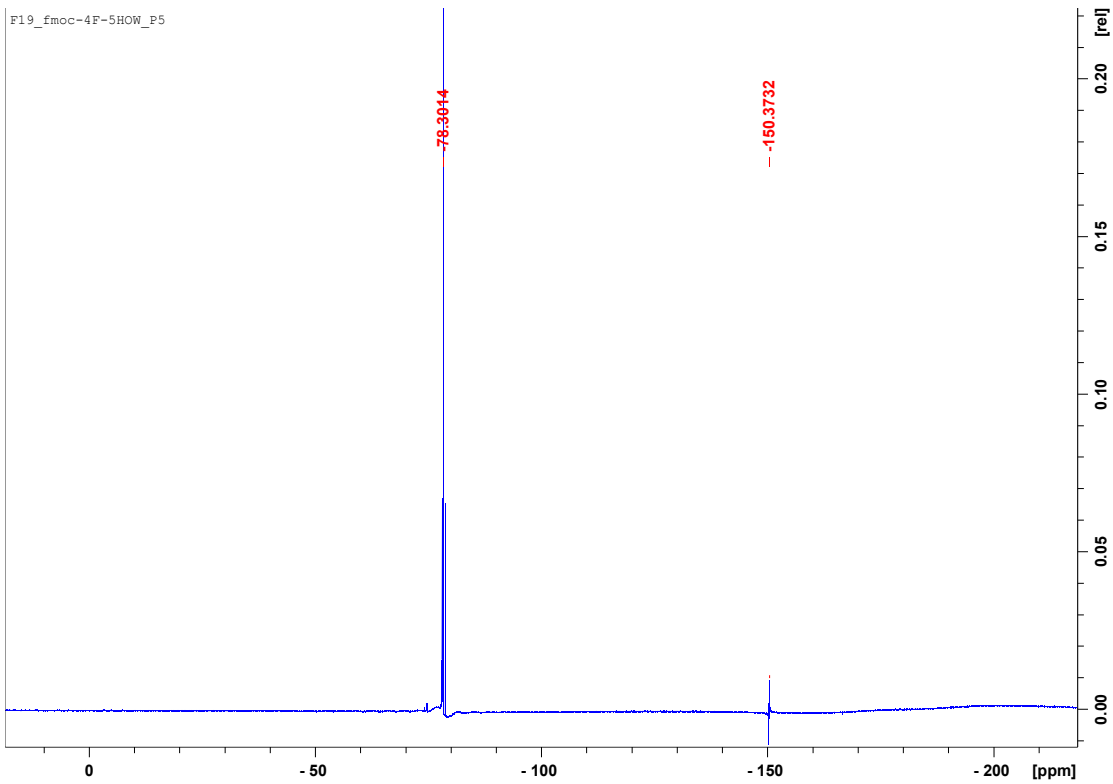


Figure 3.5. ¹⁹F NMR spectra of fmoc-4F-5HOW

Fmoc-6F-5HOW: ^1H NMR (400 MHz, DMSO), δ = 12.66 (s, 1H), 10.60 (s, 1H), 9.00 (s, 1H), 7.87 (d, 2H), 7.66 (m, 2H), 7.2-7.4 (m, 4H), 7.08 (s, 3H), 4.20 (m, 4H), 2.9-3.1 (m, 2H). ^{19}F NMR, -141.38 ppm. MS, observed: 459.52; predicted ($\text{C}_{26}\text{H}_{21}\text{FN}_2\text{O}_5$): 460.14.

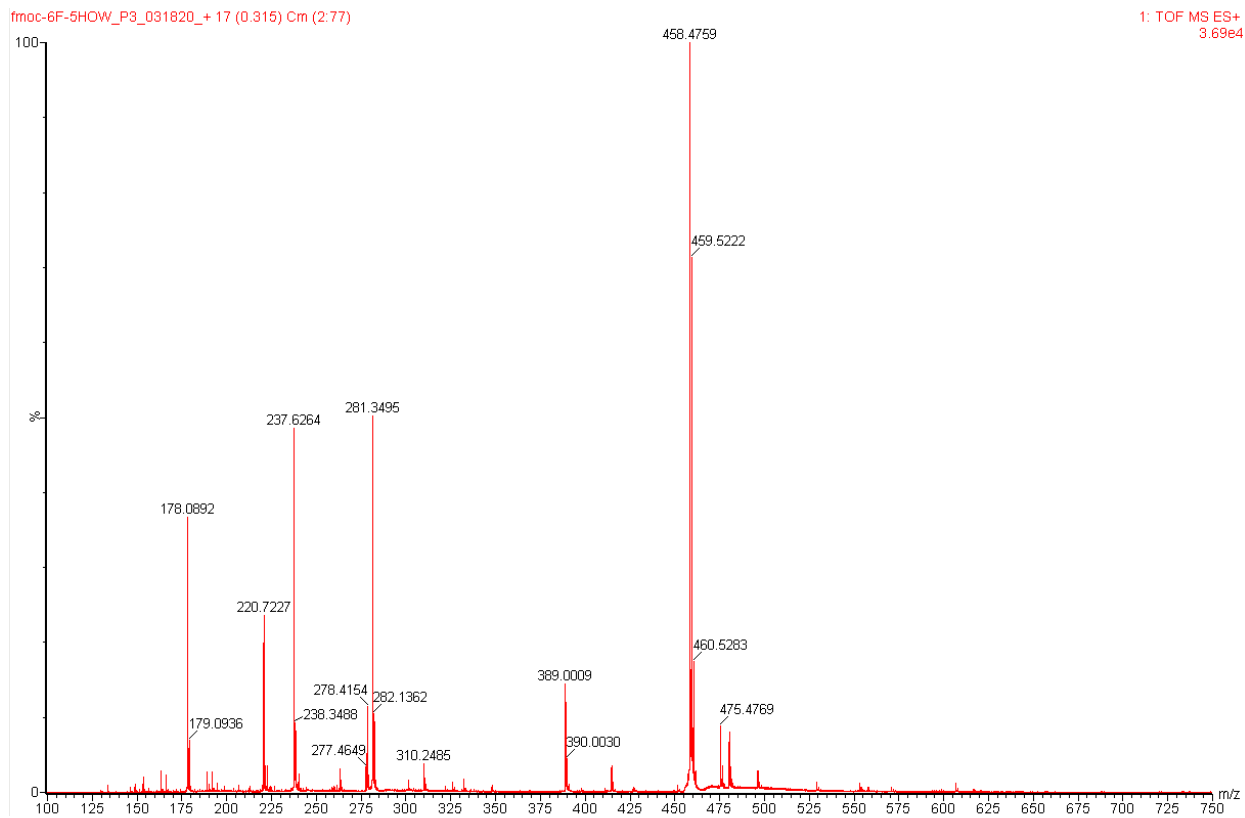


Figure 3.6. LC-MS result of fmoc-6F-5HOW

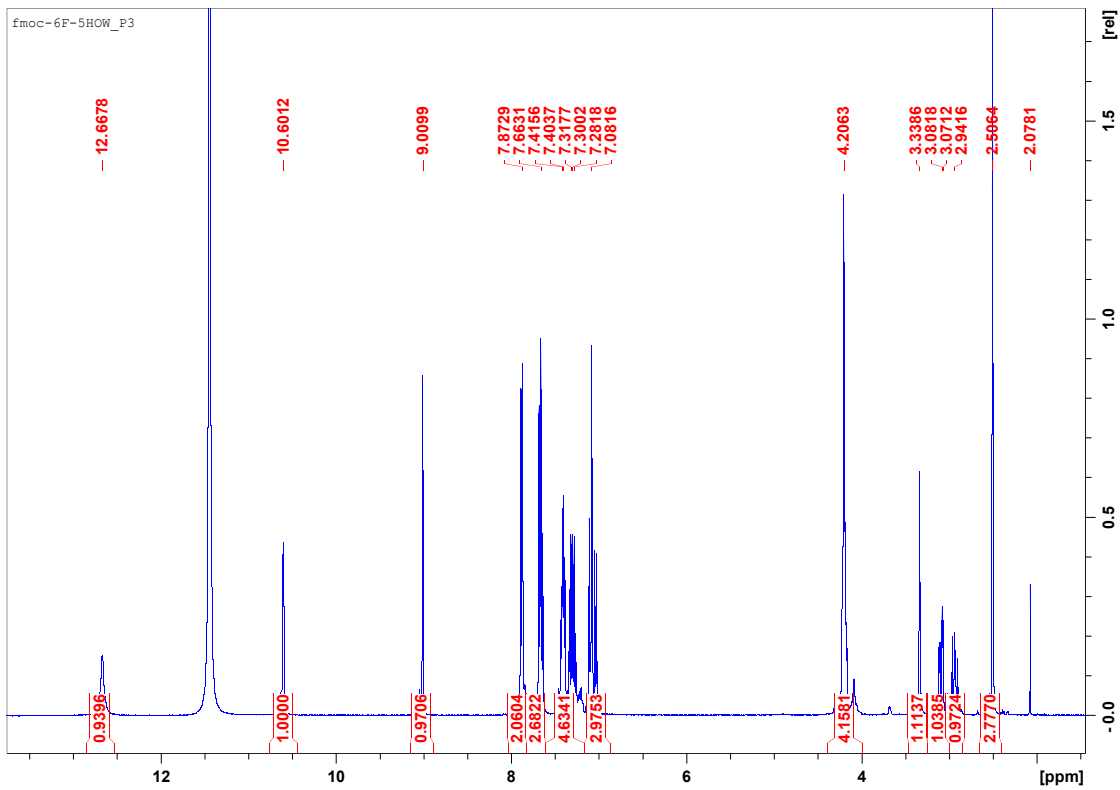


Figure 3.7. ¹H NMR spectra of fmoc-6F-5HOW

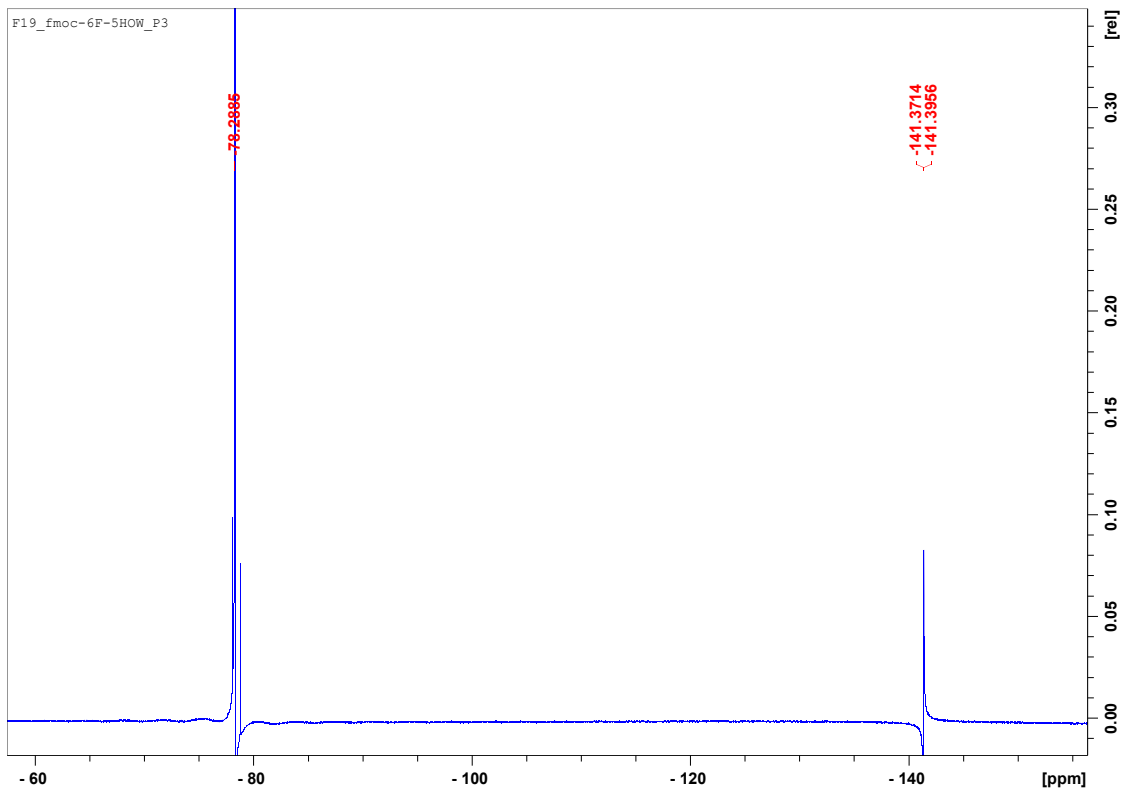
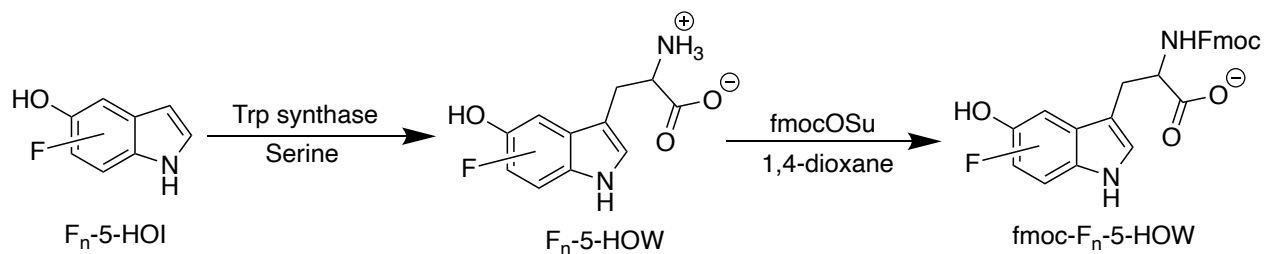


Figure 3.8. ¹⁹F NMR spectra of fmoc-6F-5HOW



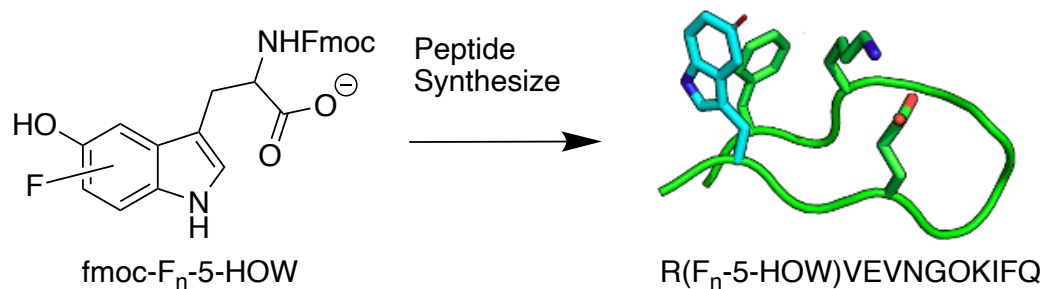
Scheme 3.2. Synthesis of unnatural tryptophan using biosynthesis approach

3.3.1. Synthesis of unnatural peptide

The 12-mer peptide, $\text{H}_2\text{N-Arg-F}_n\text{5HOW-Val-Glu-Val-Asn-Gly-Orn-Lys-Ile-Phe-Gln-CO}_2\text{H}$, was synthesized on Rink Amide AM resin using standard Fmoc chemistry, using an automated peptide synthesizer. The protocol of peptide synthesizer was below. The peptide was cleaved from the resin using a mixture of TFA/1,3-dimethoxybenzene/TES (95:2.5:2.5) and was precipitated in 20mL of cold diethyl ether. The product was purified by reverse phase HPLC (40:60:0.1 to 80:20:0.1 acetonitrile:water:TFA). The HPLC solvent was removed by lyophilization.

3.3.2. Unnatural peptide synthesis

The peptide was synthesized on Rink amide ChemMatrix resin (0.48 mmol/g). Fmoc-amino acids was coupled according to protocol A, followed by Fmoc deprotection according to protocol B. Those steps were repeated 16 times followed by coupling of Fmoc-amino acids according to protocol A and Fmoc deprotection (protocol B). The peptide was dried out and cleaved off from the resin according to protocol C and D and purified by RP-HPLC using a gradient of 60% to 20% B over 35 min (protocol E) with column.



Scheme 3.3. Synthesis of unnatural peptide

Protocol A – Peptide coupling

For automated peptide synthesis, a Syro I peptide synthesis was used. Prior to synthesis, the resin was followed by washing with dimethylformamide (DMF). Fmoc-amino acids (0.4 equiv.) and HBTU (0.4 equiv.) were each dissolved in DMF. These solutions were added to the suspension of the amino functionalized resin in DMF. The mixture was shaken for 60 min. and washed with DMF (5x).

Protocol B – Fmoc-deprotection

40% piperidine in DMF was added to the resin and the suspension was shaken for 3 min. The suspension was filtrated, and the procedure was repeated for 10 min. with 20 % piperidine in DMF. The resin was washed with DMF (7x).

Protocol C – Drying out the resin

The resin was washed by 5 mL of DCM, 5 mL of MeOH, and 20 mL of acetic acid. The solid was collected by filtration and dried out for at least 4 hours by vacuum line.

Protocol D – Cleavage off the resin

The resin was shaken for 4h in a mixture of TFA/1,3-dimethoxybenzene/TES (95:2.5:2.5) and the solution was collected by filtration. After addition of cold diethyl ether, a white solid precipitated and put into fridge for overnight. The white solid was collected by filtration and dried out.

Protocol E – Reverse-phase-HPLC purification

Acetonitrile with 0.1% TFA (A) and DI water with 0.1% TFA (B) were used as eluents. For semi-preparative HPLC a flow rate of 5 mL/min and for analytical HPLC a flow rate of 1 mL/min was used. The product was purified by reverse phase HPLC (40:60:0.1 to 80:20:0.1 acetonitrile:water:TFA). After the semi-preparative HPLC purification all collected fractions were analyzed by analytical HPLC and only pure fractions were combined. The HPLC solvent was removed by lyophilization to obtain a white foam.

3.4. Expression of tryptophan beta synthase

The plasmids encoding the evolved TrpB synthase enzymes, Tm9D8*. The plasmids encoding these TmTrpB variants provided by from Prof. Frances Arnold (CalTech). Each plasmid was transformed into *E. coli* cells. The enzymes were expressed in 800mL of DI water with 20g of 2xYT media supplemented with 800 μ L of ampicillin. The cultures were grown at 37°C to OD₆₀₀ was reached 0.8-1.0, at which point the cultures were induced with 800 μ L of 1 mM isopropyl-1-thio- β -galactopyranoside (IPTG). The temperature was adjusted to 18°C and the cultures were incubated overnight. Cells were harvested by centrifugation and the pellet was stored at -80°C until further use.

The thawed cell pellet was suspended 100mL lysis buffer containing 10% glycerol, 50 mM NaPO₄, pH 7.0, and 50mM NaCl, and 200 μ L pyridoxal phosphate (PLP). Lysis was performed by sonication. The mixture was centrifuged at 18,000 x g to remove cell debris. The supernatant was incubated at 75°C for 10 minutes and the precipitated protein was removed by centrifugation. The protein was purified with an Ni-NTA column over a linear gradient from buffer A (20mM Tris-HCl, 20mM imidazole, 500mM NaCl, pH 8.0) to buffer B (20mM Tris-HCl, 200mM imidazole, 500mM NaCl, pH 8.0). The presence of the protein was checked with UV-Vis spectroscopy and SDS-PAGE. The purified proteins (**Figure 3.9**), confirmed by gel electrophoresis, were dialyzed

overnight in 50mM KPi, pH 8.0. The proteins were concentrated, flash-frozen in liquid N₂, and stored at -80°C until needed. Typical yields were about 25 mg/L.

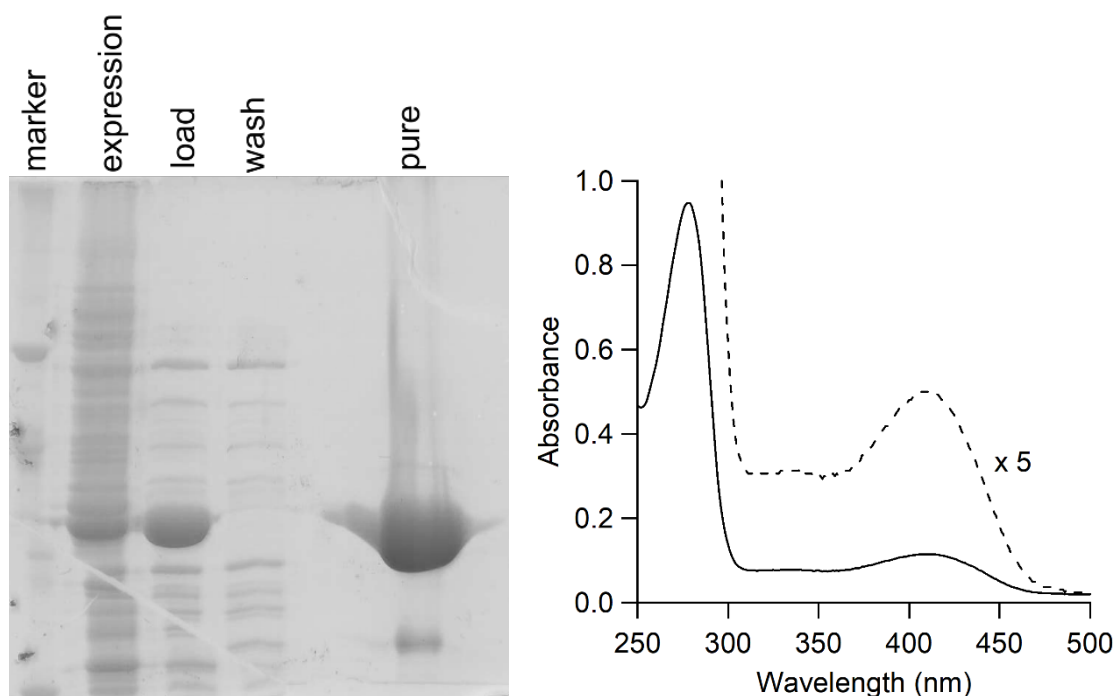


Figure 3.9. SDS-PAGE (left) and UV-vis (right) analysis of purified Tm9D8* TrpB synthase. Around 400nm signal corresponding to the PLP cofactor, bound to TrpB, is represented by the dashed line.

3.5. Incorporation of unnatural protein

Incorporation of L-5HOW in Azurin. The DNA encoding the tyrosine-deficient variant of *Pseudomonas aeruginosa* azurin (W48/Y72F/Y108F) was mutated with so that W48 was substituted for the AMBER stop codon, TAG. The pET-9a plasmid encoding this gene form Prof Schultz was cotransformed into *E. coli* with an evolved tryptophanyl tRNA/tRNA synthase pair and expressed in 2xYT media supplemented with 1 mM 5HOW. Expression was induced with 0.8mL of 1 mM IPTG once the optical density (OD₆₀₀) reached 0.9-1.2. The temperature was reduced to 18°C and incubated overnight.

Incorporation of 4F- and 6F-L-5HOW in Azurin. The fluorinated 5-hydroxytryptophan derivatives were incorporated into azurin using a Trp auxotroph of *E. coli*

W3110TrpA33(DE3)/pLysS, a gift from Prof. Bridgette Barry, and the plasmid encoding the wild type gene of azurin. A starter culture was grown in 50 mL M9 minimal media, which was supplemented with 80 mg/L of tryptophan, overnight at 37°C. Fresh 900 mL M9 media containing 80 mg/L of L-tryptophan was inoculated with 20 mL of overnight culture and incubated at 37°C until an OD₆₀₀ of 0.9-1.0 was reached. The cells were collected by low-speed centrifugation (3,000×g, 10 min, room temperature) and gently resuspended in fresh 900 mL M9 media, supplemented with 50-80 mg/4F- or 6F-5HOW. The culture was incubated at 37°C for 45 min, and azurin expression was induced with 0.8mL of 1 mM IPTG.

Azurin protein was purified from cell pellet, as previously described. The periplasmic fraction of *E. coli* cell pellet was purified by incubation (37°C, 1 h) in resuspension buffer (20 mM potassium phosphate, 2 mM MgSO₄, pH 7) supplemented with lysozyme/DNAse I. Cell debris was removed by centrifugation and the solution was adjusted to pH 4.5 using sodium acetate buffer. After removal of aggregate, copper sulfate pentahydrate was added to 10 mM. The protein solution was dialyzed overnight at 4°C in 1 mM sodium acetate, p H 4.5. Azurin was purified to

homogeneity, as assessed by a ~14 kDa band in SDS-PAGE (**Figure 3.10**) using a HiTrap SP column attached to AKTA FPLC.

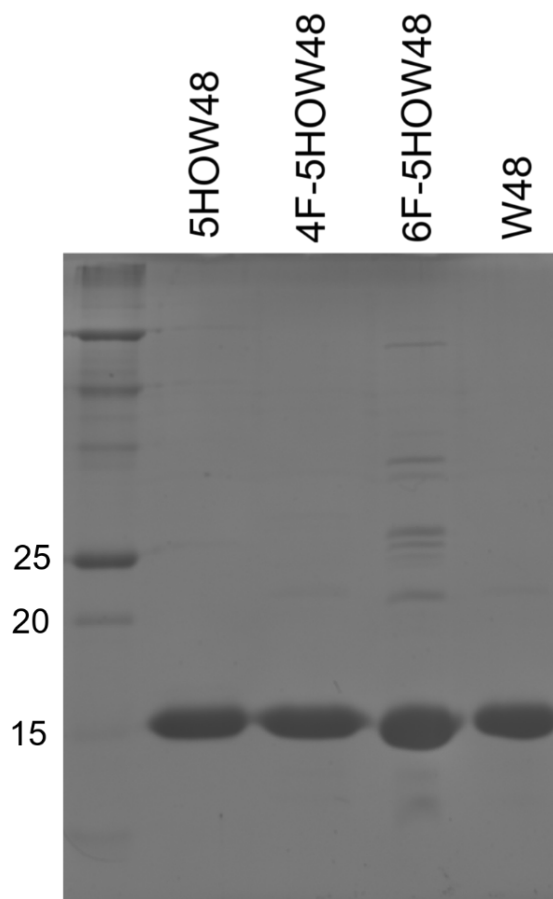


Figure 3.10. SDS-PAGE of azurin variants.

Circular Dichroism of unnatural Peptide; Peptide Folding and Stability. The folding of the beta hairpin peptide was demonstrated using CD measurements (Jasco CD spectrometer J-815). The CD spectra of the synthetic peptides were analyzed at pH 7 in 10 mM phosphate buffer and at pH 11 in borate buffer. The peptide concentration was 100 μ M. For each condition, the CD spectra of the peptides were recorded at 25°C, before and after a 90°C ‘melt’ (**Figure 3.11**). Briefly, upon completion of the first 25°C CD spectrum, the temperature was raised to 90°C and held for 5 minutes. The 90°C ‘melt’ CD spectrum was collected and then allowed to cool down to 25°C to refold the peptide. It is possible to observe high tension (HT) voltage. HT voltage is roughly proportional to absorbance. If the HT voltage goes above ~600V then the detector is saturated. The

amplitude of the spectrum will oscillate wildly. Therefore, sample is needed to dilute by buffer not to exceed 600V during the experiment, which supports that the CD trace are reliable. (**Figure 3.12**)

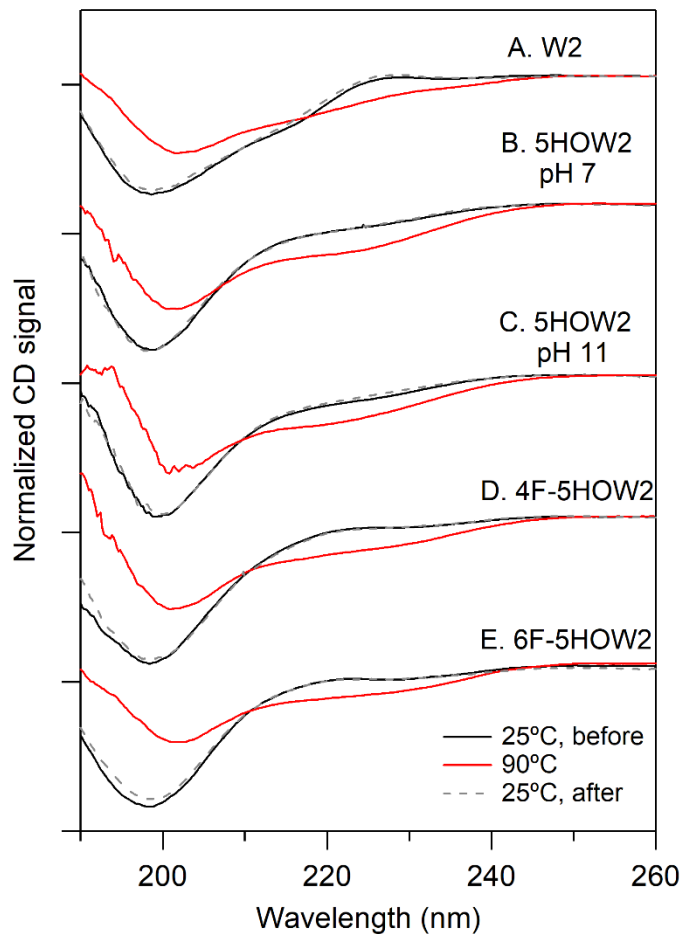


Figure 3.11. CD spectra of natural peptide and unnatural peptide.

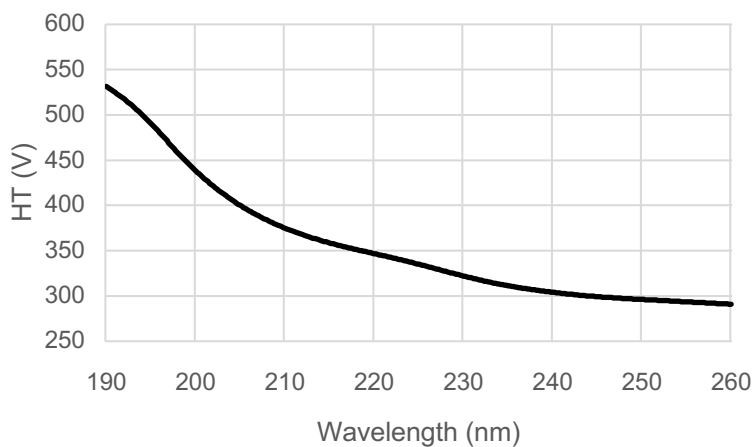


Figure 3.12. High tension voltage graph under 600V for CD spectra is reliable data.

3.6. References

1. Simon E. Kolstoe, Palma P. Mangione, Vittorio Bellotti, et al. Trapping of palindromic ligands within native transthyretin prevents amyloid formation. *Proceedings of the National Academy of Sciences - PNAS*. 2010;107(47):20483-20488.

<https://www.jstor.org/stable/25756723>. doi: 10.1073/pnas.1008255107.

2. Mąkosza M, Danikiewicz W, Wojciechowski K. Reactions of organic anions, 147. simple and general synthesis of hydroxy- and methoxyindoles via vicarious nucleophilic substitution of hydrogen. *Liebigs Annalen der Chemie*. 1988;1988(3):203-208.

<https://onlinelibrary.wiley.com/doi/abs/10.1002/jlac.198819880304>. doi:

10.1002/jlac.198819880304.

Appendix 1

Synthesis of Oleyl sulfate as an allosteric effector for lipoxygenases

A.1. Synthesis

I have successfully synthesized oleyl sulfate. To a 50 mL round bottom flask (RBF) with a 1" PTFE stir bar, 1.0 g of oleyl alcohol (3.73 mmol) was dissolved with stirring in 6 mL anhydrous pyridine. Sulfamic acid was added to the solution (0.50 g; 5.15 mmol). The reaction proceeded 1.5 hours at 95°C. The solution was quenched with 1 or 2 mL of saturated sodium carbonate solution and 20 mL of methanol, filtered solid. Solvent was rotovated off by low pressure. The desired product, confirmed by TLC (silica; 4:1 dichloromethane: ethyl acetate) and KMnO₄ stain, was purified by twice of flash chromatography using 1000 mL 4:1 dichloromethane:ethyl acetate. Solvent was removed to yield a white solid (0.32 g; 0.92 mmol; 24.6% yield). ¹H NMR (400 MHz, CDCl₃), δ = 5.32 (m, 2H), 4.01 (t, 2H), 2.00 (td, 4H), 1.61 (q, 2H), 1.27 (m, 21H), 0.88 (t, 3H).

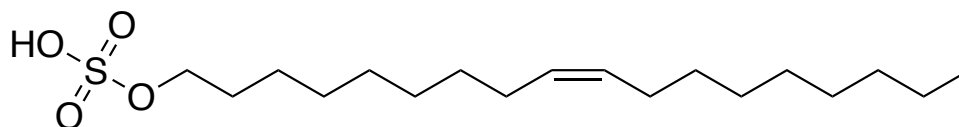


Figure A.1.1. Structure of oleyl sulfate

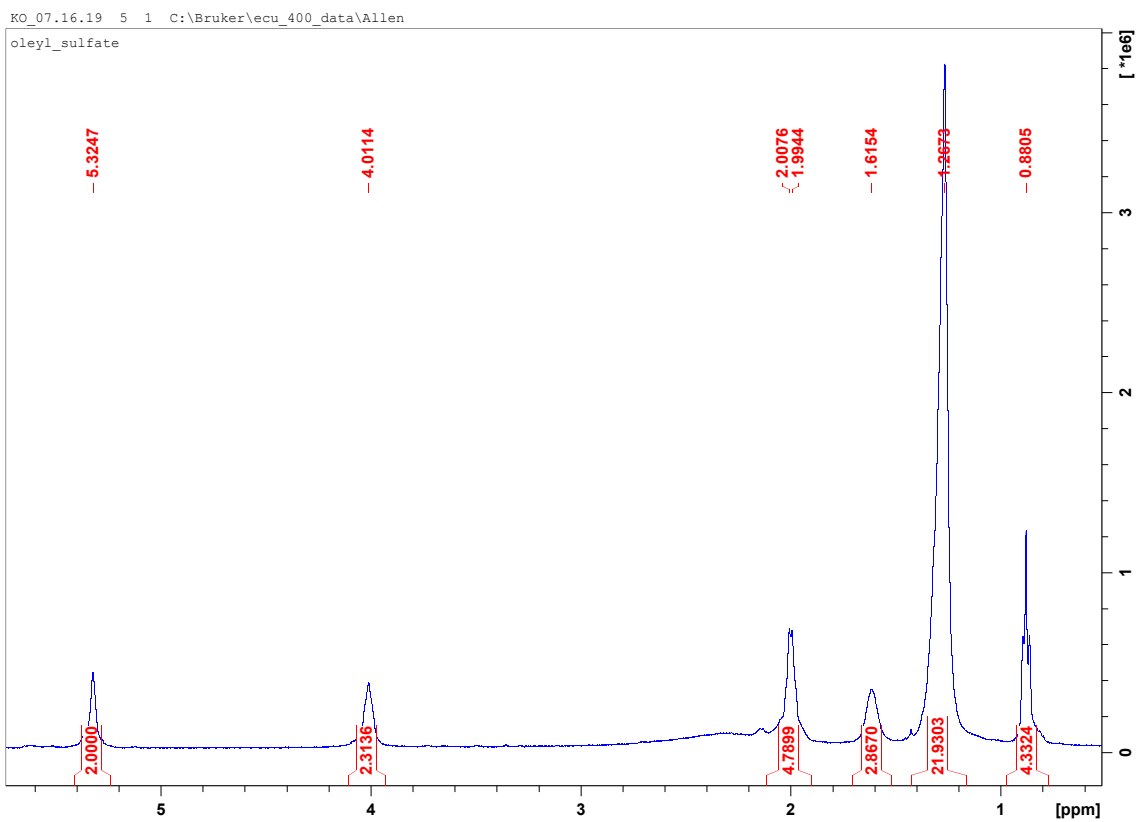


Figure A.1.2. ¹H NMR of oleyl sulfate